Tesis Doctoral
Ingeniería de Telecomunicación

Failure Detection by signal similarity measurement of Brushless DC motors

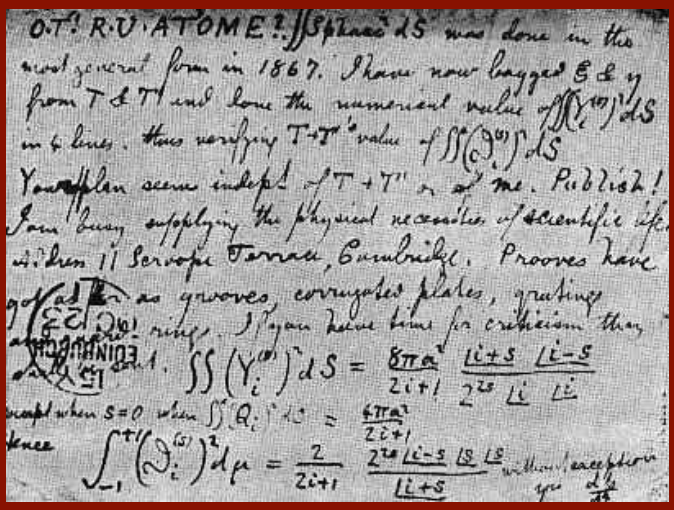

Autor: Vito Mario Fico
Director: María Ángeles Martín Prats
Director: Antonio Leopoldo Rodríguez Vázquez

Ingeniería Electronica
Escuela Técnica Superior de Ingeniería
Universidad de Sevilla

Sevilla, 2019

Tesis Doctoral
Ingeniería de Telecomunicación

Failure Detection by signal similarity measurement of Brushless DC motors

Autor:

Vito Mario Fico

Director:

María Ángeles Martín Prats

Profesor Titular

Director:

Antonio Leopoldo Rodríguez Vázquez

Responsable de Ingeniería

Ingeniería Electronica
Escuela Técnica Superior de Ingeniería
Universidad de Sevilla

2019

Tesis Doctoral: Failure Detection by signal similarity measurement of Brushless DC motors

Autor: Vito Mario Fico
Director: María Ángeles Martín Prats
Director: Antonio Leopoldo Rodríguez Vázquez

El tribunal nombrado para juzgar la Tesis arriba indicada, compuesto por los siguientes doctores:

Presidente:

Vocales:

Secretario:

acuerdan otorgarle la calificación de:

El Secretario del Tribunal

Fecha:

A Mela

Acknowledgement

Grazie **Mamma e Papà** per avermi dato sempre il vostro sostegno, andando sempre al di lá di quello che ci si aspetta da due genitori premurosi. Grazie per essere un esempio di coppia felice e per trasmetterci ogni giorno questa felicità. Vi devo molto, ma più di tutto vi devo ringraziare per aver sempre discusso e ragionato, e mai imposto. Grazie anche a mio fratello **Francesco**. Se avessi potuto scegliere io, e non il caso, avrei comunque eletto te, fra tutti, per ricoprire questo ruolo.

Grazie **Carmelina**, grazie nello specifico per l'aiuto con la tesi e, in generale, anche per tutto ciò che *non riguarda* la tesi. Durante questi lunghi mesi ho avuto da te ogni tipo di appoggio, spesso prosciugando le tue energie. Nonostante tutto, tu sei sempre stata pazientemente li a spingermi in avanti, a farmi dare il meglio, ed è principalmente grazie a te se anche questa tappa puó dirsi conclusa. Oltre a questo, ti devo molto altro.

Ti devo serenità, calma e la consapevolezza di quali sono le cose veramente importanti. Grazie per essere la mia nuova *casa* e per ogni giorno in più che mi concedi al tuo fianco, perché ti considero la miglior persona che abbia mai posato il piede su questa terra e l'unica con cui vorrei passare il resto della mia vita. La tesi, e gli sforzi che ho dovuto fare per portarla a termine sono interamente dedicati a te Carmelina, mia compagna di vita.

Ringrazio di cuore anche **Franco** per le numerose revisioni, i consigli e le discussioni illuminanti.

Este trabajo ha sido realizado gracias al soporte economico del Ministerio de Economia y Competitividad a través de la ayuda para la formación de doctores en empresas **Doctorados Industriales** del año 2014 y con ref. DI-14-06896.

Vito Mario Fico
Sevilla, 2019

Abstract

During the last years the Brushless DC (BLDC) motors are gaining popularity as a solution for providing mechanical power, starting from low cost mobility solutions like the electric bikes, to high performance and high reliability aeronautical Electro-Mechanical Actuators (EMAs). In this framework, the availability of fault detection tools suited for these types of machines appears necessary.

There is already a vast literature on this topic, but only a small percentage of the proposed techniques are developed to a Technology Readiness Level (TRL) sufficiently high to be implementable in industrial applications. The investigation on the state of the art carried out during the first phase of the present work, tries to collect the articles which are closer to a possible implementation. This selection has been carefully done with the definition of a series of rules, drawn to represent the adequate level of readiness of fault detection techniques which the various articles propose.

In the second part of the thesis, a partial demagnetisation detection method is proposed. This technique takes advantage of the asymmetries generated by the missing magnetic flux in the current to detect the failure. Both simulations and laboratory experiments have been carried out to validate the idea.

Then, the results have been examined in detail and satisfactory conclusions have been drawn.

Contents

Glossary

Detection The discovering or noticing of a fault. 12, 89

Diagnosis The identification of the cause of a fault by examination of the symptoms. XVII, 12, 89

Disturbance An unknown (and uncontrolled) input acting on a system. 12

Error A deviation between a computed value (of an output variable) and the true, specified or theoretically correct value. 12

Failure Permanent interruption of a system's ability to perform a required function under determined operating conditions. It can arise from one or more faults. Usually a failure arises when the system is working or by increasingly stressing it. 12

Fault Unpermitted deviation of at least one feature (characteristic property) of the system out of the acceptable standard condition threshold. The fault is a state of the system and can be of various types (manufacturing, assembly, maintenance, software, operators, wrong operation). It may not affect the correct functioning of the overall system. 12

Feature Extracted values from signals or process models, describing the status of the process (e.g. parameters, state variables, parity equation errors or residuals). 13

Malfunction Intermittent irregularity in the fulfilment of a system's function. It can arise from one or more faults. Usually a malfunctioning arises when the system is working or by increasingly stressing it. 12

Perturbation An input acting on a system, resulting in a temporary departure from steady state. 12

Residual A fault indicator, based on deviations between measurements and model equation based computations. 13

Symptom A change of an observable quantity from normal behaviour. 13

Acronyms

ADC Analog to Digital Converter. 75

AI Artificial Intelligence. 25–31, 35, 88, 89

BLDC Brushless DC. V, XVIII, XIX, 1, 2, 4, 16, 17, 57, 87, 89

DC Direct Current. 3, 17, 46, 95, 96

DE Dynamic Eccentricity. 10

EMA Electro-Mechanical Actuator. V, XVII

EMF ElectroMotive Force. 2, 28, 33, 35, 40, 42, 44, 46–49, 52, 53, 67, 75, 76, 91–93, 95, 96

FEM Finite Element Method. XIX, 28, 50, 60, 63

FFT Fast Fourier Transform. 27, 28

FOC Field Oriented Control. 73

HF High Frequency. 32

ITF Inter-Turn Fault. 5, 7

MCSA Motor Current Signature Analysis. 25–31, 34

ME Mixed Eccentricity. 10

MMF Magneto-Motive Force. 38

NN Neural Network. 27–29, 31, 34, 35, 84, 88, 89

OCF Open Circuit Fault. 5

PGF Phase-to-Ground Fault. 5

PM Permanent Magnet. 1

PPF Phase-to-Phase Fault. 5

PWM Pulse Width Modulation. 75, 93–96

SE Static Eccentricity. 9

SLR Systematic Literature Review. XIX, 15–17, 21, 22, 87

SNR Signal to Noise Ratio. 29

SVM Support Vector Machine. 84, 88

TRL Technology Readiness Level. V, 16, 87

Notation

pp	Pole Pairs
$degM$	Mechanical Degrees
$degE$	Electric Degrees, equal to $\frac{degM}{pp}$
i_{xc}	Normalised Cross-Correlation Indicator
i_{diff}	Normalised Averaged Difference Indicator
$triu(\mathbf{A})$	Upper Triangular part of matrix $\mathbf{A}$
$\mathbf{v}$	Vector
$\frac{\mathrm{d}x}{\mathrm{d}t}$	Time Derivative of x
$b \cdot 10^a$	Scientific Notation
$f(t)$	Continuous function
$f[k]$	Discrete function
$(f \star g)$	Cross Correlation of f with g
$\lvert a \rvert$	Absolute value of a
$\lVert a \rVert$	Norm of a
σ_a	Standard Deviation of a

Foreword and Motivation

About the Topic

With the increasing dependence on electrical apparatus, condition monitoring of electrical machines is becoming more and more important, above all when aerospace applications are involved.

An electric motor used in aerospace EMAs has to present several characteristics; it has to be light, stiff, easily maintainable and above all reliable. To improve this last point, actuator controllers were used, typically designed based on optimising performance and robustness, without considering the operational lifetime of the actuator.

Performance of flight actuators on a damaged aircraft is not as important as ensuring that the remaining actuators continue operation until the aircraft can land safely. An adequate level of reliability can be reached only using diagnostic tools. The term diagnosis indicates the process of determining by examination the nature and circumstances of a diseased condition. It can be performed collecting information provided by on-line sensors and extracting from them the characteristics that show the current condition of an equipment or a process.

This instrument is so important because an accurate and efficient means of condition monitoring and machine fault diagnosis can drastically improve reliability and stability of the plant and reduce costs, virtually leading to a system with no programmed maintenance. Statistical studies show that expected reliability can be improved up to 5-6 percentage points with the use of monitoring [8]. An ideal diagnostic procedure should take the minimum measurements necessary from a machine and by analysis extract a diagnosis, so that its condition can be inferred to give a clear indication of incipient failure modes in a minimum time.

Before developing such techniques, several studies must be carried out to understand the failure mechanism in electrical machine. At broad level the failure in electrical machine could be classified as electrical or mechanical in nature depending upon the root cause of failures. To characterise the failure nature in electrical machine it requires suitable signature acquisition and processing. Noninvasive monitoring is achieved by relying on easily measured electrical or mechanical quantities like current, voltage, flux, torque, and speed. The reliable identification and isolation of faults are still, however, under investigation as there are some open issues [9]:

- Definition of a single diagnostic procedure for identification and isolation of any type of faults
- Insensitivity to operating conditions
- Reliable fault detection for position, speed and torque controlled drives
- Reliable fault detection for drives in time-varying conditions
- Quantitative fault detection in order to state an absolute fault threshold, independent of operating conditions

It is also important for fault diagnosis of electrical machine to have strong domain knowledge, since many fields result are involved [8]. Also, in practice it is important to distinguish the fault in the machine and fault in associated system, even if sometimes it could not be easy to evaluate the safety of the whole system due to crossed interactions among all the components.

Objective and Outline of the Dissertation

The present work has been developed by having the industry needs in mind. The main objectives of this text can be summarised as:

1. Provide a study of the current literature on fault detection of BLDC motors by selecting, between the vast literature on this topic, the papers which presented algorithms closer to a possible implementation, according to the characteristics collected in Tables 2.3 and 2.4. This choice has been influenced by the author experience when dealing with fault detection papers, which often are oriented towards a more academic public and do not concentrate on the implementation. The methodology used in this work to compile the state of the art is still not diffused in the engineering world. For this reason a dedicated description has been inserted in § 2. From this study, some characteristics needed for the fault detection on electric machine have been listed and a new technique for demagnetisation detection on BLDC motors has been proposed.

2. Present an algorithm to detect demagnetisation, based on the dissimilarity between the voltages of the various electric turns of the motor due to this failure. The exposed method presents the advantages of not needing domain transforms or previous knowledge of the motor (made exception for the number of pole-pairs). Furthermore the proposed indicators are fast to be computed and require only the acquisition of motor phases voltages for a mechanical turn.

3. Confirm the hypotheses made about the effect of a demagnetisation with Finite Element Method (FEM) analysis and validate the proposed method to detect demagnetisation with experimental tests on a real motor.

The following lines present the text organisation: Chapter 1 contains the background review, with a short introduction to the BLDC motors and a not-so-short explanation of its failures' symptoms and causes. In Chapter 2 there is the literature review, carried out with the principles of the Systematic Literature Review (SLR). Chapter 3 is about the effect caused by a demagnetisation and the underlying idea of this work, while Chapter 4 presents the motor chosen for experiments and its FEM model and relative simulations, both when healthy and demagnetised. Chapter 5 shows the experiments carried out on the real motor and present the obtained results with also a possible use the fault indicators. Conclusions on results and entire work are outlined in Chapter 6.

1 Introduction

1.1 A Short Introduction to Brushless DC Motors

The use of magnetic materials in electric motors has brought, among other benefits, the improvement of the motors' reliability by resolving the problem of bringing electric current to the rotor.

The history of permanent magnet motors has been dependent on the development of the magnetic materials. The first industrial interest to manufacture permanent magnets motors arose in the 1980's as the new magnet material Neodymium-Iron-Boron (Nd-Fe-B), was developed.

The BLDC motors are nowadays one of the most diffused types, both for high and low power applications; indeed they can be found in large variety of tools and industrial machines.

According to [35] the BLDC motors give their best for powers between 1-10 kW range. Above this size the induction motor improves rapidly, while the cost of magnets works against the Permanent Magnet (PM) motor. Below it, the PM motor has better efficiency, torque per ampere, and effective power factor. Moreover, the power winding is on the stator where its heat can be removed more easily, while the rotor losses are low. The BLDC motor is also easier to control, although the inverter is similar to that required for induction motors, usually with six transistors for a three-phase system, the control algorithms are simpler and readily implemented in microcontrollers.

1.1.1 Description

These machines have a rectangular air-gap flux density and produce a trapezoidal back-emf in the stator winding (see § 3.3 for a detailed explanation). The BLDC

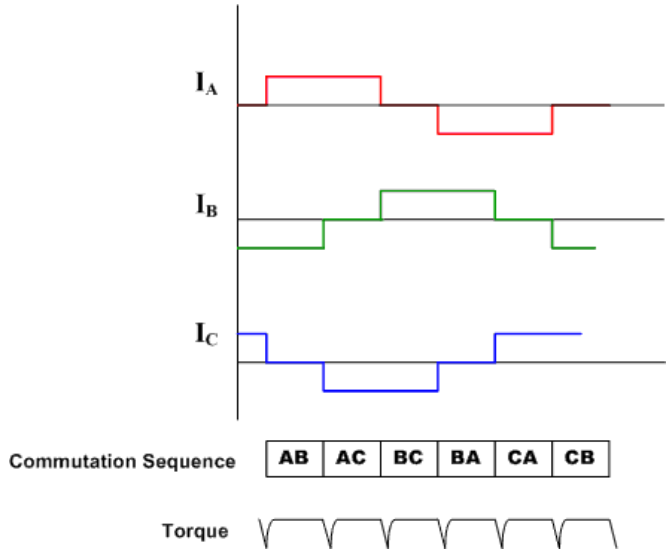

Figure 1.1 BLDC Waveforms. A, B and C represent the motor phases.

motor is specifically designed to develop nearly constant output torque when excited with six-step switched current waveforms. Figure 1.1 shows these current waveforms and the commutation sequence. It can be noted that only two phases are active at the same time. The stator windings are generally similar to those of an induction or a synchronous motor except that the conductors are distributed uniformly; that is, concentrated full-pitched windings are used to increase the width of the trapezoidal back-emf plateau region [47]. This similarity to a conventional DC motor gives the motor the name brushless DC. Despite the popularity of this name, brushless DC is actually quite misleading since the trapezoidal back-ElectroMotive Force (EMF) machine is fundamentally a synchronous AC machine and not a DC machine as the name implies. Its no-load speed is approximately proportional to the applied direct voltage, and the speed reduces somewhat with torque because of the voltage drop across the winding resistances.

The appellation *synchronous motor* is derived from the fact that the rotor and the rotating field of the stator rotate at the same speed. The rotor tends to align itself with the rotating field produced by the stator.

A permanent-magnet motor does not have a field winding on the rotor frame, instead relying on permanent magnets to provide the magnetic field against which the stator field interacts to produce torque.

Figure 1.2 shows an arrangement of a stator and a rotor of a very simple BLDC. The stator is composed by the stator core, made with a high magnetic permeability material, and the stator windings, made of a conductive wounded wire. The

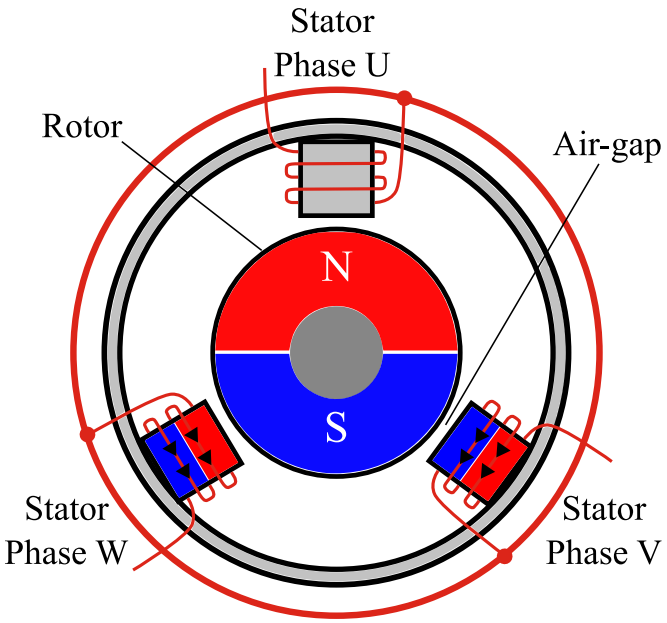

Figure 1.2 Section of a Permanent Magnets Motor.

example shows a motor with 3 phases, respectively the phase U, the phase V and the phase W.

The rotor comprises a rotational shaft and a rotor core mounted on the shaft, with two permanent magnets, each having an arc-shape cross section, so that the convex side of each permanent magnet is positioned at the outer peripheral side of the rotor core. The permanent magnets are so polarised that the north (N) and the south (S) poles are arranged alternatively. The rotor composed as described above is mounted on bearings and separated from the stator by a predetermined air-gap.

1.1.2 Basic operating principles

A Direct Current (DC) power source is connected to a switching main circuit. It is comprised of three arms; U, V and W connected into a three phase bridge configuration. Each of the arms is composed of two transistors and two diodes. Nodes of three pairs of transistors are connected to the output lines U_a, V_a and W_a which are further connected to stator windings (refer to Figure 3.7 for a scheme).

The switching main transistors are controlled by a control circuit so that the stator windings are energised for periods each of which is represented by 120 degrees. When the stator winding is sequentially energised for the respective period of 120 degrees part of the magnetic flux of the permanent magnet per pole,

it contributes to the motor torque [58].
Furthermore, a rotational position detector is provided for detecting a rotation position of the rotor, generating a rotation position signal, which is supplied to the control circuit. It provides, thanks to this information, a drive signal. In the above described permanent magnet motor, motor torque T is developed only while a current is flowing in the stator winding as it is shown in the following expression:

$$T = mKBI$$

where m is the number of phases of the stator winding, K is a constant related to the number of turns of the stator winding, B is the magnetic flux density in the air gap and I is a winding current. The above equation is particularly significant since it indicates that the current circulating in the machine is directly dependent from the produced torque. It also indicates that by electrically limiting the current, it is possible to reduce the torque in output.

In conclusion, this kind of motor is capable of operating over a much wider speed range than typical fixed speed industrial motors, but needs new materials, sophisticated electronic controls and some clever design variations.

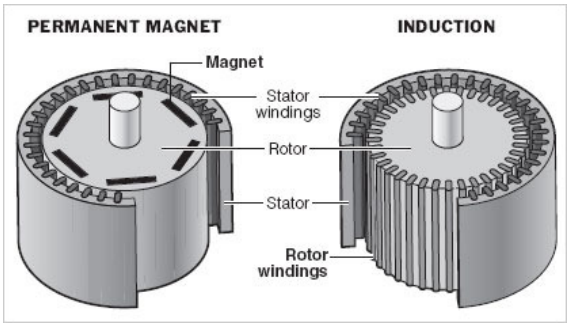

Figure 1.3 Comparison between BLDC and Induction Motor.

1.2 Failure Types

For failures classification, the main categories usually found in the literature have been used [40, 60] (bearings, stator and rotor related faults) and adapted specifically for BLDC motors:

1. Armature Faults (§ 1.2.1)
2. Permanent Magnets Faults (§ 1.2.2)
3. Eccentricity Faults (§ 1.2.3)

All the above listed failure types have severe consequences on the motor performance and useful life and they are very difficult to be detected, above all in their early stages. Following there is a list of some of the symptoms caused by these failures:

1. unbalanced line currents,
2. increased vibration level,
3. magnetic flux asymmetries,
4. decreased performances, increased losses and heating.

The statistics about the failure distribution are not very precise ([40], [2], [12], [41]) but it can be said that more or less 80% of failures are shared between armature faults and eccentricities faults and the data collected during the present work are in accordance with this statistics.

In the following subsections the failures type are described in detail.

1.2.1 Armature Faults

Description

The armature faults refer to all those failures happening in the winding, usually in the form of a short-circuit. According to its position, it can be classified as:

- Inter-Turn Fault (ITF) (Figure 1.4c)
- Phase-to-Phase Fault (PPF) (Figure 1.4b)
- Phase-to-Ground Fault (PGF) (Figure 1.4c)
- Coil-to-Coil Fault (Figure 1.4a)

This failure usually starts with a ITF and evolves into a more serious PPF and PGF. An Open Circuit Fault (OCF) can also happen in the winding, although it is more common in the motor driver.

Causes

The winding insulation is subjected to multiple stresses and all contributes to its ageing and failure mechanism. According to [59] these factors can be divided into:

Thermal Temporary rise of temperature in conductors and thermal cycling can cause degradation of mechanical and electrical properties of insulation materials. From the first appearance of the short-circuit, the rise of temperature in the shorted link, further degrades the insulation, causing the failure to worsen faster.

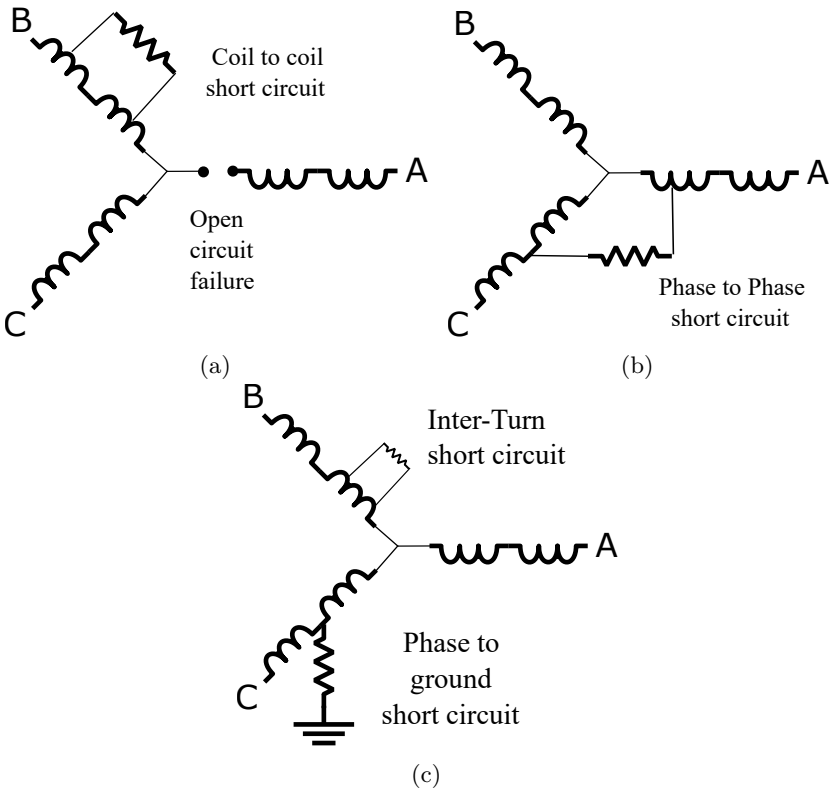

Figure 1.4 Types of armature faults: Coil to coil (a), Phase to phase (b), Inter-Turn and Phase to ground short circuits (c).

Electrical Electrical (internal or external) phenomena like *partial discharges*, *surface tracking* and *transient voltages* can cause local degradation of the insulation material. Even if the insulating materials operate below their inherent breakdown strength, the electrical ageing of insulation can occur as the result of the presence of faults in the material. For example gas voids arising from imperfect impregnation can cause partial discharges.

Mechanical Mechanical stresses like abrasions during operation or manipulation of the machine are a common source of insulation degradation.

Environmental If the machine operates in an harsh environment or the due precautions have not been taken, it can accelerate the machine degradation at any level. Indeed the contamination of insulation systems by water, oils or chemicals can cause insulating materials to degrade mechanically, electrically or thermally.

Specific Symptoms

The ITF is one of the most subtle failure in the motor because it evolves very fast into a more serious damage but it is very difficult to be detected when it is at an incipient stage. The following list collects the symptoms which can be seen in case of a winding failure, but it has to be considered that their appearance and intensity strongly depend on the fault magnitude:

1. unbalanced line currents,
2. increased vibration level,
3. decreased performances, increased losses and heating.

1.2.2 Permanent Magnets Faults (partial or complete)

Description

The permanent magnet faults include all those pathological conditions that modify the air-gap flux. The failure can be symmetrical (although this is very uncommon) or not, causing different effects as increased phase currents and cogging torque, reduced average torque, unbalanced magnetic pull, increased vibrations level and operating temperature.

Causes

The magnetic properties of a permanent magnet derive from the fact that its magnetic domains are aligned. There are certain circumstances that can cause the loss of that alignment and, with it, some or all of its magnetic field. The causes which bring to demagnetisation are principally two and will be briefly resumed following.

Every magnetic material has a characteristic temperature known as the *Curie temperature*. Heating a magnet up to reach this temperature is the primary method to cause the loss of its magnetic properties. In fact at this temperature the thermal agitation is greater than the resistance of the magnetic domains, causing a loss of the magnetic properties. A magnet can be partially demagnetised placing a magnetic load upon it. This effect can be understood if we look at the second quadrant of the hysteresis curve of the magnetic material in object, also called as the demagnetisation curve. This curve shows the response of the magnets delivered flux into the space around it (B) to the demagnetising force (H) imposed on the magnet (Figure 3.1a).

To assess the performance of the magnet material in a given situation, the user should calculate the ratio of B/H, by superimposing a line on the demagnetisation curve, as shown in the Figure 1.5 for a B/H ratio of 0.8.

Always referring to Figure 1.5, it is possible to notice that there are present

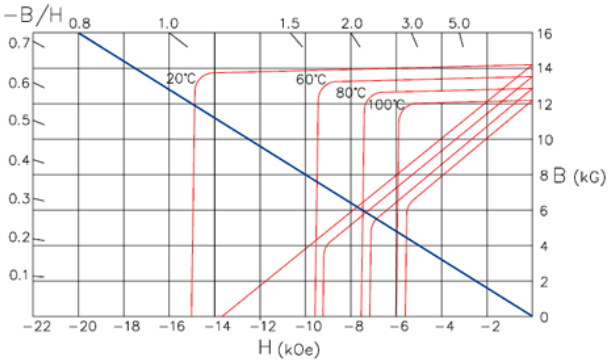

Figure 1.5 An Example of Demagnetisation Curve.

a set of red lines which are the demagnetisation curves. They are varying with temperature and they have a bend, also called *knee*.

If the blue line, which shows the working condition of the magnet, crosses above the knee in the curve, then the magnet is operating in its safe linear region and should perform as expected. If the magnet's load line is below the knee on the curve, the magnet can be demagnetised.

It is also important to notice that the knee gets higher with increasing temperatures, which reflects the material's increasing vulnerability to demagnetisation at higher T.

Other demagnetisation causes may include high short-circuit currents produced by inverter or stator faults, and less commonly the ageing of the magnet itself.

The magnets can be also mechanically damaged by corrosion or cracks, causing partial demagnetisation (chipped magnet Figure 1.6) or even disintegration at high speed.

Specific Symptoms

A partial demagnetisation causes unbalanced magnetic pull, that turns in noise and vibration increment or, in the worst case, it can cause the stator and rotor to rub, leading to total machine loss. The authors of [52], following the work in [47] demonstrated through a *Finite element analysis* of a rotor with 3 pole pairs and a partial demagnetised magnet, that the characterising fault frequencies can be localised using the formula:

$$f_{dmg} = f_e \cdot \left(1 \pm \frac{k}{P}\right) \tag{1.1}$$

Figure 1.6 A chipped magnet.

where f_{dmg} is the fault frequency, f_e is the electrical supply frequency, k is an integer that represents the harmonic, and P is the number of pole pairs.

Unlike the faulty bearing case, in the flux disturbance case, the stator current does not contain any new spectral content at the rotating frequency. This is true since the relative permeability of the magnets is almost equal to one which is, in turn, a value very close to the magnetic permeability of the air.

Thus, the windings do not experience a larger air-gap for a missing magnet piece. However, due to the missing magnet piece, there is a step change in the flux density curve around the rotor [30]. This results in a frequency component at the rotating frequency; i.e. at the harmonic number calculated with equation (1.1).

1.2.3 Mechanical Faults (bearing failure and eccentricity)

Description

Small eccentricities are normally present in all motors, but when they become large, they can cause rub between stator and rotor due to the unbalance of radial magnetic forces. In a well centred machine, the rotor axis is aligned with the stator bore and the centre of rotation is the same as the geometric centre of the rotor-stator group. Both when the rotor is stationary or when it's running the airgap is the same all along the circumference.

As shown in Figure 1.7, air-gap eccentricity can occur in the form of static, dynamic or mixed eccentricity.

Static Eccentricity (SE) The rotor geometric centre coincides with the rotation centre, but it is displaced from the stator geometric centre. The position of the minimum radial air-gap length is fixed in space.

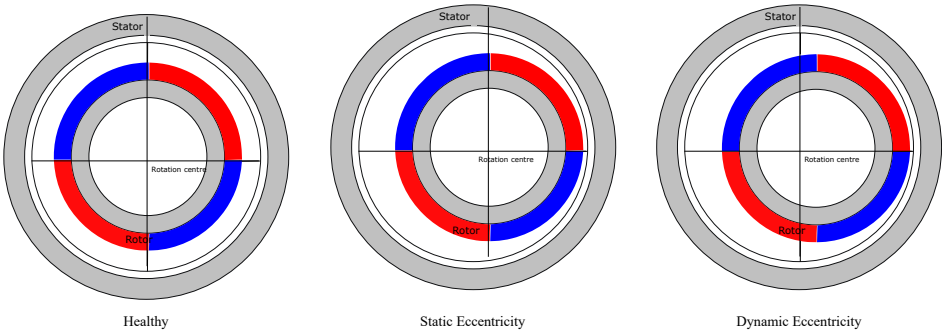

Figure 1.7 Types of Eccentricity.

Dynamic Eccentricity (DE) The rotor geometric centre is displaced from the stator geometric and rotation centre. The minimum air gap revolves with the rotor, i.e. is a function of the rotor angular position.

Mixed Eccentricity (ME) The rotor geometric centre, the rotation centre and the stator geometric centre are in different positions.

In the case of static eccentricity, there is a steady pull in one direction, while in the case of dynamic eccentricity the magnetic pull rotates at the same speed of the rotor.

Causes

The rotor eccentricity is mainly caused by the bearing wear or also by the bearing housing deformation. Those events can be caused by the normal internal operating stresses (vibration, inherent eccentricity, and bearing currents), and by different external causes such as:

- contamination, corrosion caused by pitting or by water, acid, etc., sanding action of hard and abrasive minute particles
- improper lubrication; which includes both over and under lubrication causing heating and abrasion,
- improper installation of bearing, e.g. by forcing the bearing onto the shaft or in the housing; indentations in the raceways (brinelling); mechanical ovalisation of the rotor core.

The different faults which can occur in a bearing can be classified according to the affected element:

- outer raceway defect,
- inner raceway defect,
- ball defect.

A faulty bearing could have a small hole, a pit or a missing piece of material (or a combination of them) on each of the components.
Other causes of dynamic eccentricity include bent shafts and mechanical resonances at critical speeds.

Specific Symptoms

A motor affected by mechanical failures presents:

- magnetic flux asymmetries,
- increased vibration and noise levels,
- increased heat generation.

Regardless of the failure mechanism, defective rolling element bearings generate mechanical vibrations at the rotational speeds of each component. These characteristic frequencies can be calculated using equations (1.2) and depend on bearing geometry and on rotational speed of the machine. Mechanical vibration analysis techniques are commonly used to monitor these frequencies in order to determine the condition of the bearing.

$$\begin{aligned} f_o &= \frac{n}{2} f_r \left[1 - \frac{BD}{PD} cos\beta\right] \\ f_i &= \frac{n}{2} f_r \left[1 + \frac{BD}{PD} cos\beta\right] \\ f_b &= \frac{PD}{BD} f_r \left[1 - \left(\frac{BD}{PD}\right)^2 cos^2\beta\right] \end{aligned} \tag{1.2}$$

where,

f_o: frequency introduced by a outer race defect,

f_i: frequency introduced by a inner race defect,

f_b: frequency introduced by a ball defect,

BD: balls' diameter,

PD: pitch diameter,

β: contact angle between spheres and cage,

n: number of balls or rollers,

f_r: relative revolutions per second between inner and outer race.

Above parameters are sketched in Figure 1.8 for a better understanding. Studies conducted in [54] demonstrate that bearing's damages produces changes in stator current too. Indeed, since ball bearings support the rotor, any bearing defect will

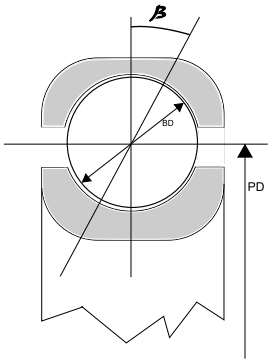

Figure 1.8 Bearing's parameters.

produce a radial motion between the rotor and stator of the machine, modifying the machine's air-gap. This dynamic air-gap eccentricity affects the inductance of the machine, leading to variations in stator current frequencies f_{bng} which are predictable if supply frequency f_e and vibration frequencies of the bearing are known. This relation is shown in equation (1.3):

$$f_{bng} = f_e \pm \ m \cdot f_v \tag{1.3}$$

where m is an integer representing the harmonic, ... and f_v is one of the characteristic vibration frequencies calculated in equation (1.2).

1.3 Nomenclature

By going through the literature, the terminology in this field appears non-uniform. This is due to the fact that Fault Detection and Diagnosis is usually distributed over many different disciplines. The definition of the following terms is specified in the glossary section and is based on [25]. This terminology will be used along the entire document.

- Fault
- Failure
- Malfunction
- Error
- Disturbance
- Perturbation

- Feature
- Residual
- Symptom

From the description it is possible to draw the relationship between faults, failures and malfunctions (Figure 1.9).

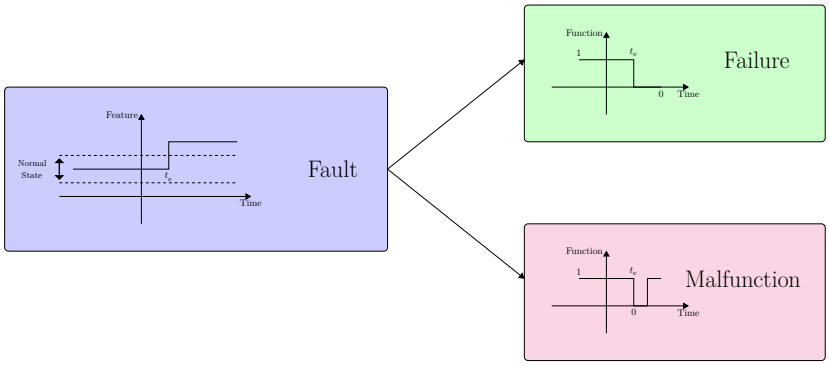

Figure 1.9 Scheme of the relation between faults, failures and malfunctions.

2 Literature Review

The first step of a research work is certainly the bibliographic review on the specific theme, in order to understand not only its actual state, but also its evolution. In the field of engineering, and in particular for aerospace engineering, traditional (or narrative) revision is preferred, in which the authors decide the papers to include in the review based on their profound knowledge and experience and giving a personal vision and interpretation of the topic.

The systematic literature review (SLR) is a very rigorous and reliable standardised scientific methodology, mainly characterised by its objectivity. It is used with excellent results in many areas, including psychology, medicine and in recent years also in software engineering.

It consists of three sequential phases, each of which is subdivided in turn into sub-phases, as detailed below:

1. Planning the review
    - identification of the need
    - research questions
    - review protocol
    - evaluating protocol
2. Conducting the review
    - selection of primary studies
    - study quality assessment
    - extraction and synthesis of data
3. Reporting the review

- specifying dissemination mechanisms
- formatting the main report
- evaluating the report

In the following, all the steps undertook to perform a SLR on **high TRL fault detection techniques for BLDC motors** will be presented. The guidelines presented in [28] for software engineering and [23] for systems and automation engineering have been taken into account; in particular from the latter many ideas and suggestions have been followed when using and evaluating the protocol.

2.1 Aim of the Research

The aim of this review is to indicate which techniques are currently being used successfully for motor fault detection and diagnosis and to provide the industry with some high readiness level and tested techniques. In this view, many of the *inclusion* (Table 2.3) and *exclusion criteria* (Table 2.4) have been formulated to focus the research on those techniques with demonstrated failure detection performances at various operation points and easily *automatable* or already automated.

Another important point considered in the review has been the possibility to embed in the motor body, the hardware needed for fault detection. Indeed, although most papers focused on the detection by using already measured variables (current, voltage and speed) some authors developed failure detection techniques by analysing images from external cameras or very sensitive (an bulky) accelerometers. Those techniques are suitable to be implemented only in very particular applications.

2.2 Planning

The first step of the systematic review consists in *planning*, which is the foundation of the entire revision. It is at this stage that the main tools are developed, such as the Boolean function, the inclusion and exclusion criteria, the choice of the different databases in which to carry out the research and above all the development and evaluation of a protocol that regulates all the phases.

The need to undertake a systematic review, arises first of all because the research topic is very wide and a rigorous method was needed to correctly extract the needed information. As said, in the engineering field this type of methodology is not usual because, even by being scientific and rigorous, it is difficult and complicated to carry out. Currently there is no systematic review on the fault

detection techniques for brushless DC motors, and in reality there is not even a traditional revision so detailed on the chosen theme[1].

2.2.1 Research questions

Once the concrete topic has been identified, there are some criteria that help to clearly formulate research questions. Among the most used criteria in other sectors there are the criteria called PICOC (Population, Intervention, Comparison, Outcome, Context).

In this case, just some of these criteria have been used to formulate and process the questions that this SLR is trying to answer. In the final section of the review, defined as reporting, there is a sub-section called Discussion (§ 2.4.1) where the relative answers are discussed and analysed.

The questions formulated for the present work are listed below:

RQ.1: Which are the most common failures of BLDC motors?

RQ.2: Which parameters are used for fault detection in BLDC motors?

RQ.3: Which type of failure can be detected by each technique?

RQ.4: Which technique requires less computational power?

RQ.5: Which technique requires less sensors?

RQ.6: Which technique gives the best results for each type of failure?

2.2.2 Review protocol

The revision protocol is nothing more than a set of rules and criteria to be followed during all the stages, in order to reduce the bias and make the SLR as objective as possible.

A very important aspect to be considered for the SLR is the clarity wherewith the protocol is exposed and elaborated, as at least two persons are involved in the review drafting. A common, but very time consuming, approach consists in the implementation of the SLR by two independent persons, who carry out the part of the conducting and reporting separately and then compare and discuss the obtained results. Another method, that is the one used in this work, is that a person performs all the phases individually and a second person randomly checks some data, as for example, some of the rows of the features tables (Table 2.7, 2.8, 2.9).

[1] Should be clarified that this sentence is referred to the reviews taking into account the readiness level of the technique.

One of the basic steps of the protocol is the creation of a Boolean function that comprehensively includes all the terms related to the chosen theme, including all the synonyms and terms that may be related to the words of interest for the topic. To carry out this research based on keywords, it is appropriate to deeply read about the theme to detect which words are most frequently used by the authors.

The Boolean function created for this work is as follows:

((("brushless DC" OR "permanent magnet electrical") AND (motor OR machine)) OR BLDC OR PMSM)
AND
(((condition OR health) AND monitoring) OR ((diagnosis OR detection) AND (fault OR failure)))

The first part of the Boolean function defines the type of motor, while the second one defines the detection of the defect.

A difficulty encountered during the research is that the different bibliographic databases are not prepared for this kind of revision, as they do not allow certain researches or to search in certain fields of the papers. Indeed, the Boolean function based research was carried out in the title, in the abstract and in the keywords of the papers.

Due to the research restrictions of the databases, as specified in [23], and thanks to the good coverage of the editorials obtained shown in Figure 2.1, the following databases have been used:

- IEEE Xplore Digital Library
- Scopus
- ACM Digital Library
- Science Direct
- Web of Science

Once the research questions have been identified and the relative Boolean function created, it must be introduced in the different bibliographic databases, adapting it according to the search language of each database. In this work, the research has been carried out by searching only in the abstract, title and keywords of the papers, obtaining a total of 2746 items until of **May 2018**, as detailed in Table 2.2.

Another important step of the *Planning* phase is the formulation of the *inclusion* and *exclusion* criteria. This criteria are very important, as they are used as objective rules for the selection of the studies that can become part of the review.

Table 2.1 Databases coverage with respect to the content of the publishers: *IE=IEEE, IT=IET, PE=Pegamon-Elsevier, ES=Elsevier Science, WB=Wiley Blackwell, TF=Taylor & Francis, SP=Springer, SI=SIAM Publications, OX=Oxford University Press, KO=Korean Inst. Electrical Eng., SA=Sage Publications, AS=ASME, MP=Microtome Publications [23].*

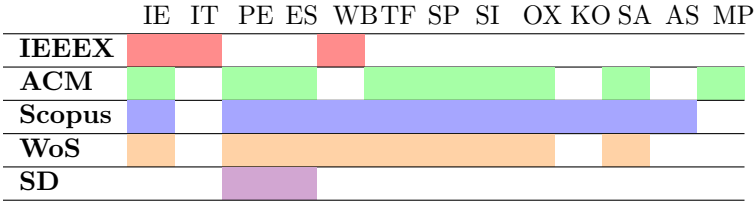

Table 2.2 Studies obtained by each database.

Database	Studies
Web of Science (WoS)	590
IEEE Xplore (IEEEX)	842
ScienceDirect (SD)	600
ACM Digital Library (ACM)	17
Scopus	697
	2746

For a paper to become part of the review it *must respect* all the inclusion criteria, presented in the Table 2.3 and *must not contain* any of the exclusion criteria presented in the Table 2.4.

The inclusion criteria are all related to the research theme itself, i.e they explain exactly what is expected to be found in an article in order to be accepted. Among the exclusion criteria, however, there are some points that are proper to the systematic review, such as the criterion that excludes all secondary studies or grey literature (books, book chapters, PhD thesis, reviews, etc.). In this way it is ensured that the selected articles have already passed through a peer-review process.

In addition to all these tools, needed to reduce the 2746 papers coming from the Boolean function search (see Table 2.2), it is needed to define some guidelines on how to carry out the selection of the studies and finally how to extract the data considered important from every paper.

The author decided to extrapolate the following features from each article:

- Data of the article (e.g. author, year of publication, etc.)
- The type of failure

Table 2.3 Inclusion Criteria.

Num.	Description
1	Shall propose at least one detection technique (a parameter or an index that clearly and uniquely identifies the failure or an automatic detection algorithm)
2	The proposed technique should not be restricted to a particular machine (number of phases, etc)
3	To be applied the technique shall not need special set-ups, configurations, loads or motor manoeuvres
4	The technique shall have been tested at various operation points (different speed or loads or a combination of both)
5	Characteristics of the detection and diagnosis algorithm: a. The algorithm (or index) shall have been tested with success for at least one of the following cases: • Different levels of the same failure, demonstrating coherence (simulation or test on real motor) • On different real motors, demonstrating coherence • On simulation and then real motor, demonstrating coherence • Capability do discern between different failures b. The paper shall demonstrate that the algorithm is capable to discern between healthy and faulty

Table 2.4 Exclusion Criteria.

Num.	Description
1	Grey literature and secondary studies (reviews, books, PhD theses)
2	Non English written papers
3	Duplicated studies
4	Full paper not available
5	Does not present tests or simulations
6	Uses big sensors, not embeddable in the motor (cameras or similar)
7	Does not concentrate on the topic

- The type of technique used
- The type of sensors used
- If it presents experiments or simulations
- If the algorithm has been tested at different speeds or loads
- If the algorithm has been tested in dynamic or stationary conditions

2.3 Conducting

The second phase of the SLR is the conducting and is mainly divided into three parts: the selection of primary studies, a study quality assessment and finally the extraction and synthesis of data for each paper.

The main objectives of this phase are:

- to significantly reduce the large number of studies that have been obtained, by using the inclusion and exclusion criteria,
- to extract a features table in which the main characteristics of each article are highlighted.

2.3.1 Selection of primary studies

To guide the selection process of primary studies, it is very common to use the PRISMA [36] (Preferred Reporting Items for Systematic Reviews and Meta-Analyzes) method . The method consists of 27 points and a flow chart built with the aim of making the whole process simpler and more ordered.

Referring to Figure 2.1, of the **2746** papers initially selected, the first screening takes place eliminating the duplicates, which in this case turn out to be **1111**; this is due to the fact that many databases share some publishers, as shown in the Figure 2.1. It is advisable to use a software (Mendeley, Zotero, JabRef, etc.) to automatically detect the duplicates. Once the duplicates have been removed, it is necessary to take care of the grey literature as for some databases was not possible to exclude it during the research.

At this point the next step consists in reading the title, abstracts and keywords and in applying the inclusion and exclusion criteria to the remaining **1635** articles. Often, by only reading these fields it is not clear whether the article meets all the required requirements or not, so it is necessary to read the whole article. This problem is mainly due to the fact that in the field of engineering in general, there is no normalisation of rules to create these fields, as it exists in other sectors such as medicine or psychology.

The papers that definitively become part of the review are **37** (see Figure 2.1), a much smaller amount if compared to the initial 1635, as shown in Figure 2.2.

In conclusion, from the total amount of articles, 307 of them have been accepted for full paper review and finally, only 37 papers met the selected criteria for being included in the revision. They will also be used to try to answer to all the questions previously formulated.

The *Conducting* phase is certainly the most difficult phase and where perhaps more time has been spent compared to the whole systematic review, since 1635 papers have been carefully analysed. For many of these, the full-text review was

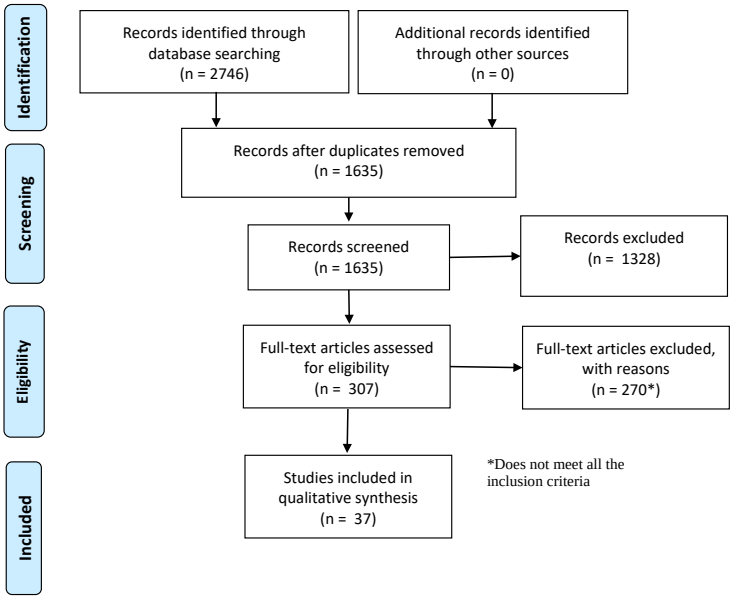

Figure 2.1 PRISMA flowchart.

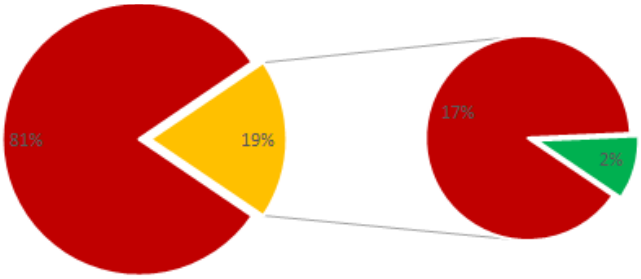

Figure 2.2 Paper inclusion statistics.

necessary to verify and ascertain whether all the criteria had actually been met or not.

At this stage it's also where another reviewer comes in. As said there were two possibilities: either to revise all 1635 papers and then compare the results, or randomly choose some paper and review them to see if the SLR has been carried out correctly.

2.3.2 Study quality assessment

For the current systematic review **37** papers have been chosen.

A quality study has been carried out on them, i.e all the points presented in Table 2.5 have been analysed. The results of this quality assessment are shown in the Table 2.6.

Table 2.5 Checklist for quality assessment.

	Question	Score
Q1	Is the problem presented clearly?	Yes/Partly/No
Q2	Is the methodology used presented clearly?	Yes/Partly/No
Q3	Is there a discussion of the results?	Yes/Partly/No
Q4	Does it answer to the presented problem(s)?	Yes/Partly/No
Q5	Has it been cited by many authors?	Cites
Q6	Has it been published in a journal or conference proceeding?	Journal / Conference

Table 2.6 contains only qualitative information related to the selected articles. Some answers may be more or less objective, as for example if the problem or methodology have been presented clearly, while others are completely objective, as for example the cites of each article with respect to year of publication or if it has been published in a journal or in a conference.

2.3.3 Extraction and synthesis of data

In order to extract and synthesise the data of the selected papers, a summary table (Tables 2.7, 2.8, 2.9, 2.10) has been created. It has to be pointed out that the data presented in this work is updated to **May 2018**. In this tables are listed the more important characteristics of the papers related to the research topic.

- Year of publication;
- The category of the detected fault. This field can be one or more of the following items: armature faults, mechanical faults or permanent magnet faults;
- The class of the technique used for the detection. The main categories have been selected to be:
  - Electromagnetic field monitoring, search coils, coils wound around motor shafts (axial flux-related detection),
  - Temperature measurements,
  - Infrared recognition,
  - Radio-frequency (RF) emissions monitoring,

Table 2.6 Checklist for quality assessment for the selected papers.

	Q1	Q2	Q3	Q4	Q5	Q6
[37]	Y	Y	Y	Y	1	Journal
[4]	Y	Y	P	P	0	Conference
[10]	Y	P	P	P	0	Conference
[20]	Y	P	Y	Y	0	Conference
[21]	Y	P	Y	Y	1	Conference
[33]	Y	Y	Y	Y	13	Journal
[42]	Y	N	N	P	2	Journal
[44]	Y	Y	P	Y	1	Conference
[62]	Y	P	Y	Y	7	Journal
[17]	P	Y	P	Y	7	Journal
[26]	Y	P	P	Y	5	Conference
[34]	Y	Y	Y	Y	21	Journal
[38]	Y	P	Y	Y	18	Journal
[55]	Y	Y	Y	Y	15	Journal
[2]	Y	Y	Y	Y	5	Journal
[5]	Y	Y	P	Y	4	Journal
[12]	Y	Y	P	Y	5	Conference
[32]	Y	Y	P	P	3	Conference
[39]	Y	P	Y	P	30	Journal
[11]	P	N	Y	Y	20	Journal
[18]	Y	P	N	Y	19	Conference
[41]	Y	P	Y	Y	24	Journal
[53]	Y	P	P	P	70	Journal
[61]	Y	P	Y	Y	68	Journal
[3]	Y	P	P	Y	5	Conference
[31]	N	Y	Y	Y	38	Journal
[6]	Y	Y	Y	Y	37	Journal
[27]	Y	Y	Y	Y	35	Journal
[43]	Y	P	P	Y	6	Conference
[14]	Y	P	Y	Y	45	Journal
[13]	Y	P	Y	Y	84	Journal
[46]	Y	P	P	Y	14	Conference
[50]	P	P	P	P	3	Conference
[51]	P	P	P	P	13	Conference
[49]	P	P	P	P	10	Conference
[7]	P	Y	P	P	18	Conference
[48]	Y	Y	Y	Y	108	Journal

– Noise and vibration monitoring,

– Chemical analysis,

  - Acoustic noise measurements,
  - Motor Current Signature Analysis (MCSA),
  - Model, Artificial Intelligence (AI), and neural-network-based techniques,
  - Parameters estimation,
  - Other (specify).

  The last item has been left if some technique cannot be classified into the previously listed categories.

- The sensor(s) needed for the failure detection technique implementation,
- If the demonstration of the effectiveness of the proposed detection techniques has been carried out with simulation and/or experiments,
- If the simulations and/or experiments have been carried out under different working conditions, such as different speeds and/or different loads,
- If the proposed technique is capable of working during changes in load and/or speed or the working conditions should be kept stationary,
- Other limitations and/or advantages. This feature is the only one that is subjective, but it contains useful information that cannot be collected in the other features.

The papers are presented in chronological order. This is usually done when performing a systematic review to put in evidence the major number of articles on the topic published during the last years. It is also useful to show if there is some clear change in research trend about one of the considered parameters.

2.4.3 Important references about Electric Motors

Apart from the papers listed in the previous sections, the present study has benefited from several works on electric motors, specifically for what concerns the working principles, the mathematical modelling and the physical behaviour of the machines themselves [16, 19, 35, 29, 22].

4 FEM Analysis

In this chapter, the motor used in the experimental part of the work will be described in details; most of its characteristics have been directly observed while others have been conveniently obtained. The aim of this procedure is to set-up a FEM model of the motor as accurate as possible, in order to properly compare the simulation results with experimental data.

4.1 Motor Description

4.1.1 Overall Characteristics

The motor used is a BR2804-1700K_v, a 14-pole 12-slot low-power BLDC outrunner motor. Its specifications are listed in Table 4.1.

Table 4.1 BR2804-1700K_v Datasheet.

K_v	1700 RPM/V	**Stator Inner Diameter**	3.5 mm
Rated Voltage	11.1 V	**Stator Outer Diameter**	22 mm
No Load Current	0.6 A	**Length of Stator Core**	4.4 mm
No Load Speed	18000 RPM	**Rotor Inner Diameter**	25.6 mm
Nominal Current	5.6 A	**Rotor Outer Diameter**	27.6 mm
Nominal Speed	12540 RPM	**Length of Rotor**	4 mm

The 14 magnets are square shaped with dimensions of 4 mm x 4 mm x 1.6 mm and with an unitary weight of 0.19 g.

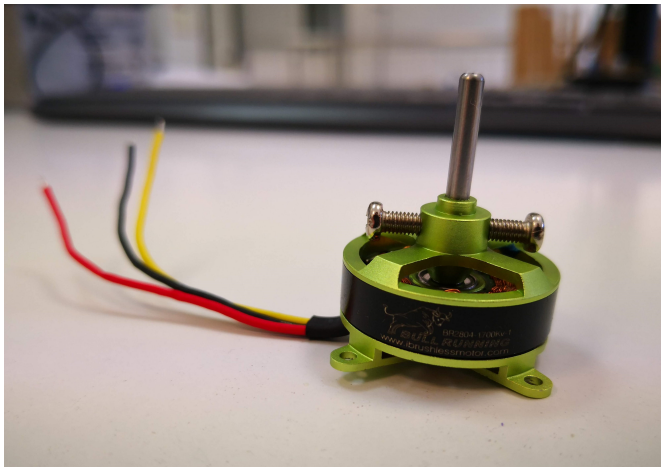

Figure 4.1 BR2804-1700K$_v$ Motor.

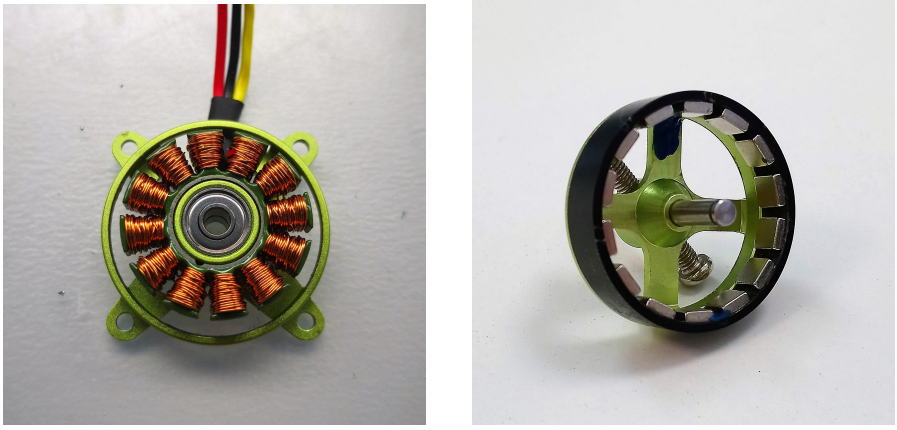

(a) (b)

Figure 4.2 Motor parts: Stator (a) and Rotor (b).

4.1.2 Winding

The motor winding is clearly visible in Figure 4.2a. In order to obtain all the parameters needed to fully describe the winding properties, it has been necessary to unroll the wire around the stator teeth. Before doing this, through an ohmmeter the phase to phase resistance has been measured, resulting equal to 0.223 ohm as the Figure 4.3 shows.

A single terminal is composed of four wires which separate in groups of two and go to two adjacent teeth when entering the stator. Following one of these

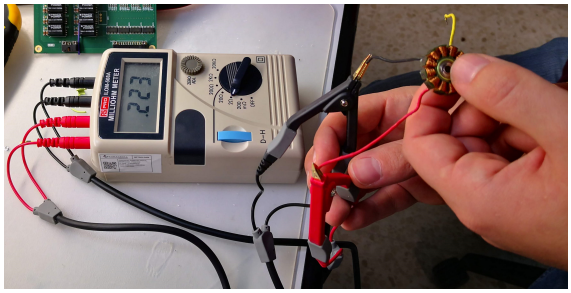

Figure 4.3 Phase to Phase resistance measured through an ohmmeter.

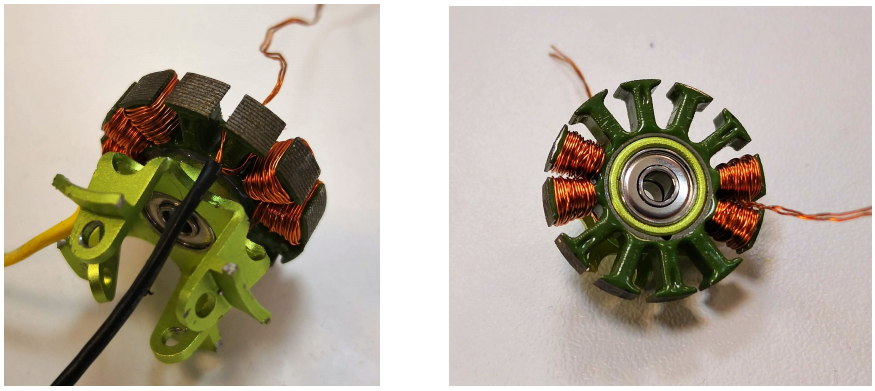

(a) (b)

Figure 4.4 Unrolling motor winding; rear view (a) and single phase wound on the stator (b).

branches, it has been noticed that the conductors wind up consecutive stator teeth in opposite directions, i.e. clockwise and counterclockwise, then they move four slots forward and roll around the next stator tooth according to the last direction used, i.e. counterclockwise and clockwise (Figure 4.4b clarifies this arrangement).

The conductors are then soldered together with two more wires from another motor phase. The scheme described so far is identical to the one shown in the right side of the Figure 3.6; therefore, it has been possible to conclude that the analysed motor is Delta connected. A simple scheme for this connection is illustrated in the Figure 4.5, where it is also highlighted that each phase is composed of two wires.

A coil is made of 22 turns of two wires each; this leads to state that there are 44 conductors per slot. A single wire diameter is equal to 0.24 mm. It has also been found out that the stator is covered with a thin insulating layer (the green material visible on the stator teeth in the Figure 4.4b); its thickness is approximately equal to 0.1 mm.

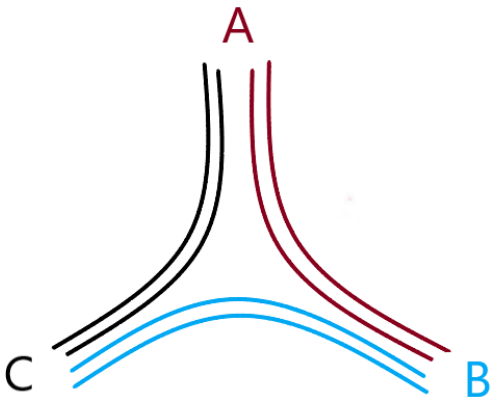

Figure 4.5 Delta Connection Scheme for the motor BR2804.

Furthermore, it is worth noticing that from the phase to phase resistance measurement it is possible to evaluate the single phase resistance value, being true for a Delta connected motor the relation reported in Table 4.2. The three phase resistances have been assumed to be equal.

Table 4.2 Relation between phase to phase resistance and single phase resistance in a delta connected motor, assuming that phase resistances are equal.

$R_{1-2} = \frac{2}{3}R$	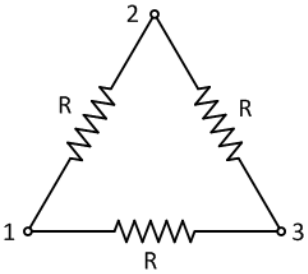

Table 4.3 summarises the winding parameters.

4.2 FEM Model

The basic model of the motor has been realised in the RMxprt package of Ansys Electromagnetic Suite and then exported to Maxwell 2D to perform a FEM

Table 4.3 Summary of Motor Winding Parameters.

Connection	Δ
Turns per Coil	22
Wires per Phase	2
Conductor per Slot	44
Single Wire Diameter	0.24 mm
Phase to Phase Resistance	0.223 Ohm
Single Phase Resistance	0.33 Ohm

analysis. All the information given in § 4.1 have been used as an input to the software.

4.2.1 RMxprt

RMxprt offers numerous templates for different type of electric machines; this allows to easily enter design parameters and verify performance data.

In Table 4.4a are listed the parameters used for the analysis. Stator and rotor have been built using geometrical data mentioned in Table 4.1, while other significant input data are reported in Table 4.4b. The resulting machine is shown in Figure 4.6a.

Table 4.4 Motor Design Parameters.

Rated Power	45 W
Rated Voltage	11.1 V
Rated Speed	12500 RPM
Frictional Loss	0.2 W
Winding Loss	0.2 W
Transistor Drop	0.3 W
Diode Drop	0.2 W

(a) Motor Analysis Setup.

Stator Steel Type	iron
Rotor Steel Type	iron
Magnet	XG128-120
Minimum Air Gap	0.175 mm
Rotor Stacking Factor	0.95
Pole Embrace	0.85

(b) Rotor and Stator Input Data.

A winding model fitting the one shown in Figure 3.6 has been created; it is displayed in Figure 4.6b, where coils have been connected to show in-slot (lower part of the slot) and out-slot (upper part of slot) connections. Moving in the

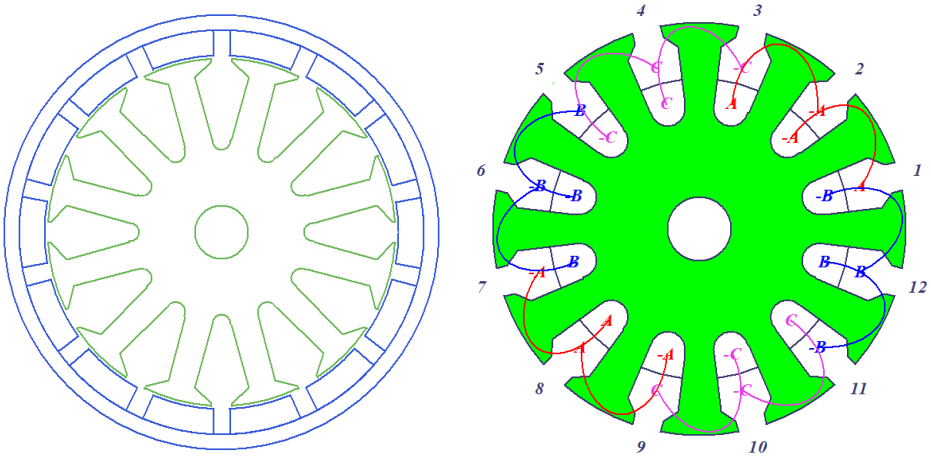

(a) Machine Geometry. (b) Winding Layout.

Figure 4.6 RMxprt Model.

$\mathbf{H_{s0}}$	0.2 mm
$\mathbf{H_{s1}}$	1 mm
$\mathbf{H_{s2}}$	4 mm
$\mathbf{B_{s0}}$	1.4 mm
$\mathbf{B_{s1}}$	3.5 mm
$\mathbf{B_{s2}}$	1.3 mm

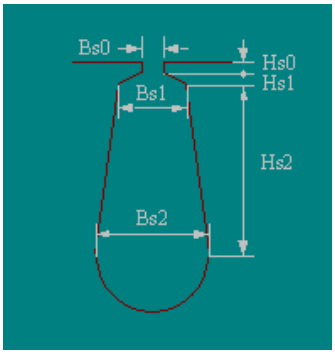

Figure 4.7 Slot Design Parameters.

clockwise direction around the stator, a coil wound clockwise has in the in-slot a positive phase while a negative phase indicates a coil wound counterclockwise.

Slot design has been obtained inserting the input quantities shown in the Figure 4.7. Furthermore, the slot and wire insulation has been set according to the measurements; in particular, a wire with 0.239 mm diameter has been selected, to which an insulation wrap of 0.01 mm has been added, to be consistent with the measured wire diameter.

4.3 FEM Simulations

The model design built in the previous section has been exported to Maxwell 2D, where a transient FEM analysis has been carried out. Time variation of the stator currents, torque and speed can be calculated, besides the induced voltages on stator winding.

The first simulation has been performed for 10 ms, with the motor running at the rated speed of 12500 RPM, as indicated in Table 4.4a. This corresponds to complete 2.084 mechanical turns in the given time.

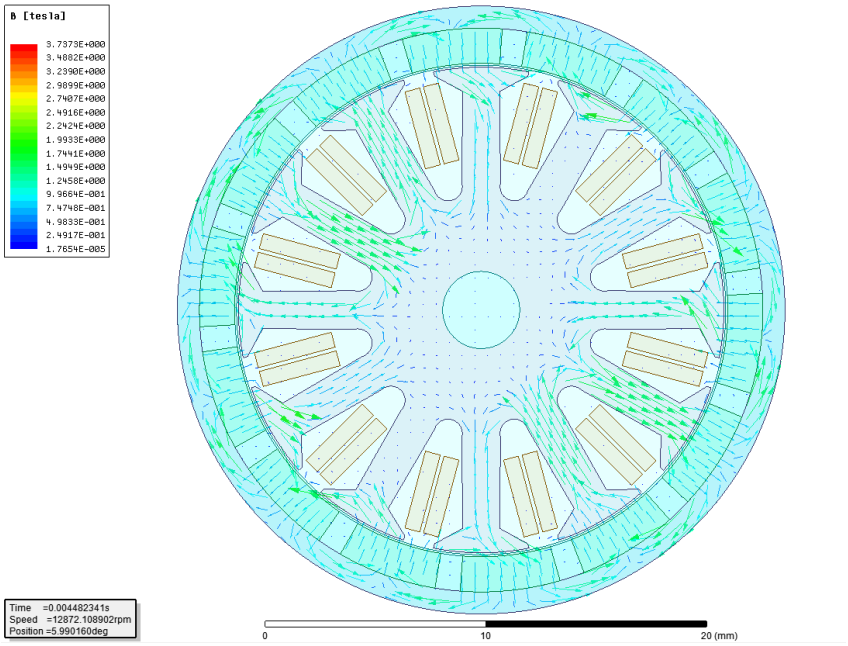

Figure 4.8 Distribution of the Magnetic Flux Density in BR2804 Motor.

In Figure 4.8 and Figure 4.9 are respectively reported the distribution and the magnitude of the magnetic flux established inside the different motor parts. It is possible to notice from the winding diagram that B and C are the active phases at the considered time; moreover, the symmetry of magnetic field can be appreciated, with a maximum magnitude of $\mathbf{B}$ approximately equal to 1.6 T in the stator teeth.

Figures 4.10 to 4.12 show time variation of torque, winding currents and winding induced voltages at 12500 RPM for 10 ms. The curves are very regular and exhibit the expected behaviour. The torque average value is equal to 32 mNm, while currents reach peaks of 4.5 A in absolute value. The induced voltages show a

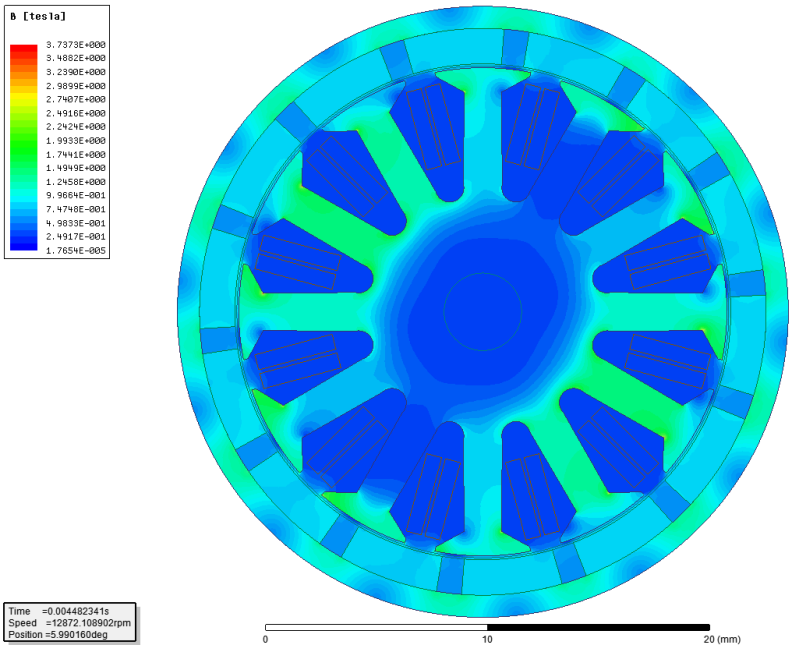

Figure 4.9 Intensity of the Magnetic Flux Density in BR2804 Motor.

trapezoidal shape with spikes of 11.43 V, due to the inductive response of the winding to commutation.

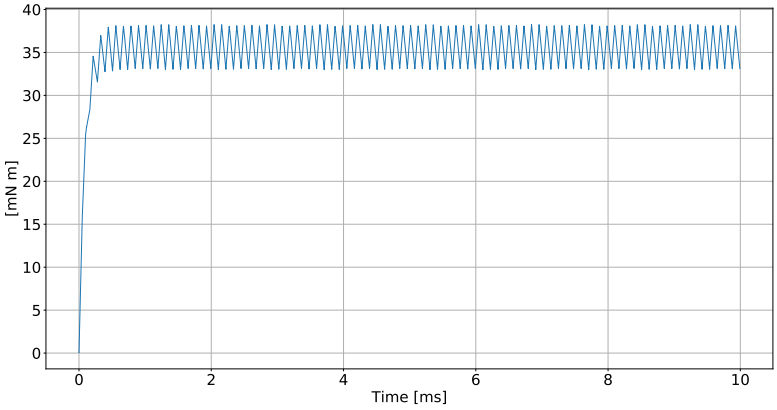

Figure 4.10 Time variation of torque in BR2804 Motor at 12500 RPM, 10 ms simulation.

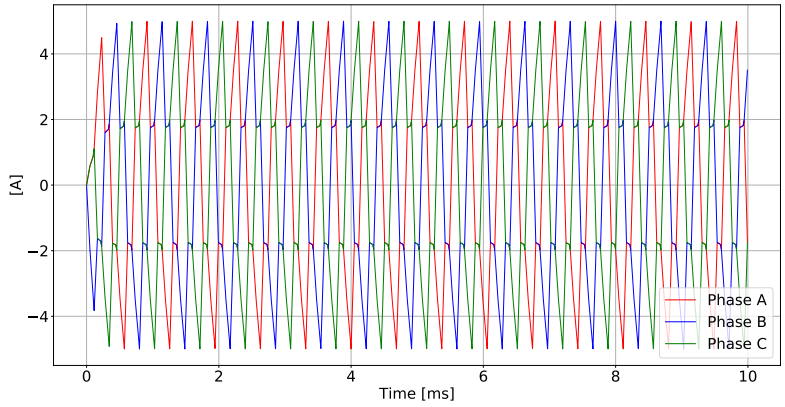

Figure 4.11 Time variation of winding currents in BR2804 Motor at 12500 RPM, 10 ms simulation.

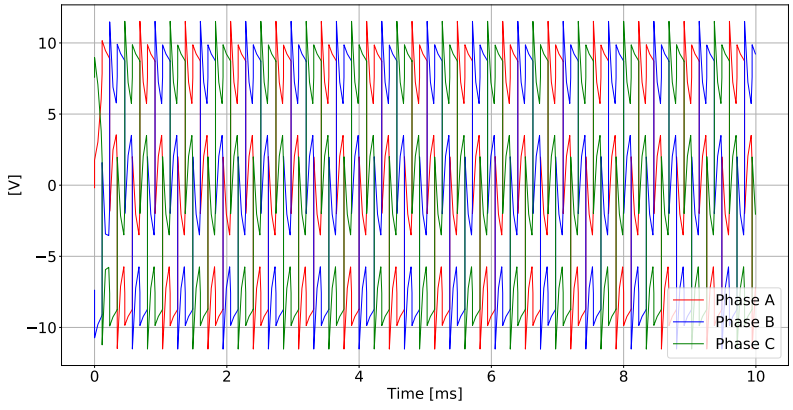

Figure 4.12 Time variation of winding induced voltages in BR2804 Motor at 12500 RPM, 10 ms simulation.

4.4 FEM simulations with demagnetisation

The model described in § 4.2 has been modified to simulate a partial motor demagnetisation. The partial demagnetisation has been reproduced by conveniently changing the magnetic properties of one magnet. In details, the magnet coercitivity magnitude has been reduced from -560000 Am to -10000 Am.

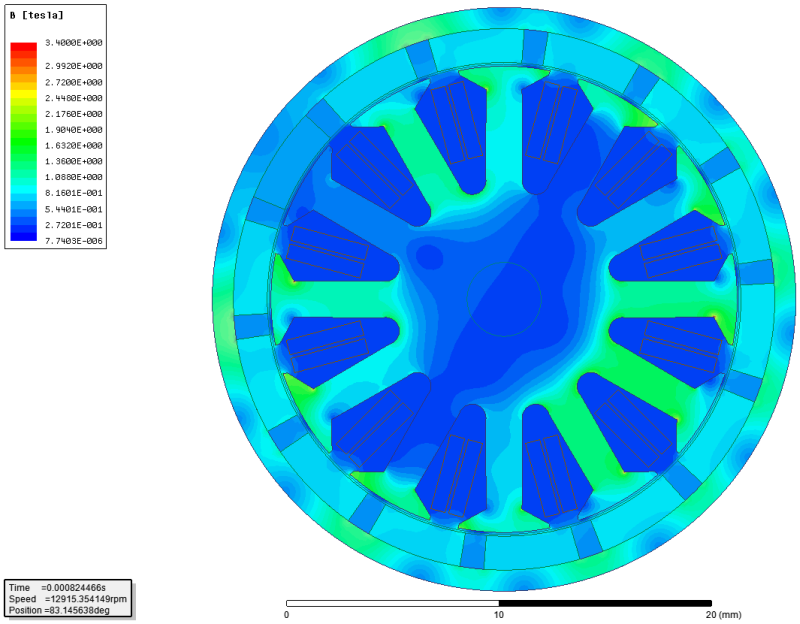

Figure 4.13 Intensity of the Magnetic Flux Density in BR2804 Motor with a demagnetised magnet at 12500 RPM.

Figure 4.13 shows the results of the simulation; it is clearly visible a remarkable flux reduction corresponding to the damaged magnet and a resulting asymmetry in the magnetic field distribution.

Time variations of torque, winding currents and winding induced voltages have been compared with the corresponding values obtained for the healthy motor, previously shown in § 4.3; in order to highlight the differences, only one phase (phase A) current and induced voltage have been shown.

In Figure 4.14 time variation of phase A induced voltage along a single mechanical turn has been displayed; even though the curve keeps a trapezoidal shape, a non uniformity of its distribution is visible, with also a certain variability of values. This result has been described in § 3.4 and § 3.6.1; in particular, Figure 3.5 shows

a behaviour of the induced voltage for a damaged motor very similar to the one resulting from simulation.

The change in back-EMF values is too small to be fully appreciated; a more evident result has been shown in Figure 4.15, where the phase A flux linkage along a mechanical turn has been reported. It is clearly visible a flux linkage reduction corresponding to the damaged magnet.

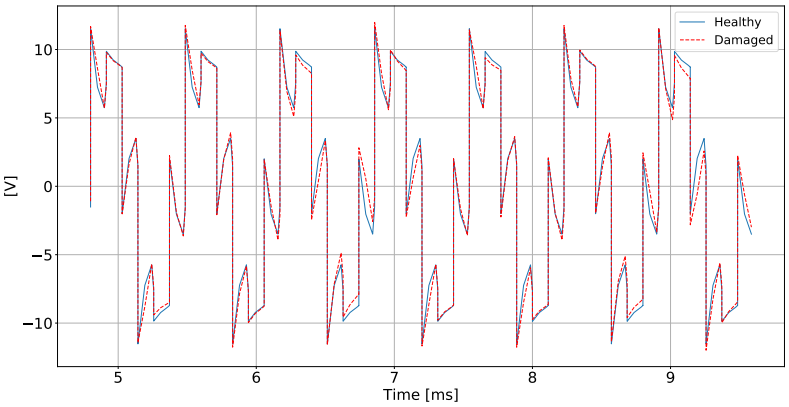

Figure 4.14 Comparison between time variation of phase A induced voltage in BR2804 healthy motor and with a demagnetised magnet along a mechanical turn, at 12500 RPM.

As a consequence, it is possible to see an increase of correspondent winding current value for the same complete mechanical turn, as shown in Figure 4.16 and in Table 4.5, where the RMS value of the three current phases has been reported and compared with the corresponding one for the healthy motor. This last result was also anticipated in § 3.5.

Table 4.5 Current Data Comparison along a mechanical turn.

Three Phases Current RMS Value		
Healthy	*Damaged*	*Percentage Increase*
1.367 A	1.593 A	14.21%

Figure 4.17 shows the torque-time characteristic of the motor with a defected magnet along a mechanical turn; as described in § 3.6.1, torque distribution appears to be unbalanced along mechanical turns, with abnormal torque ripples. This is a direct effect of the different current distribution. The mean torque value

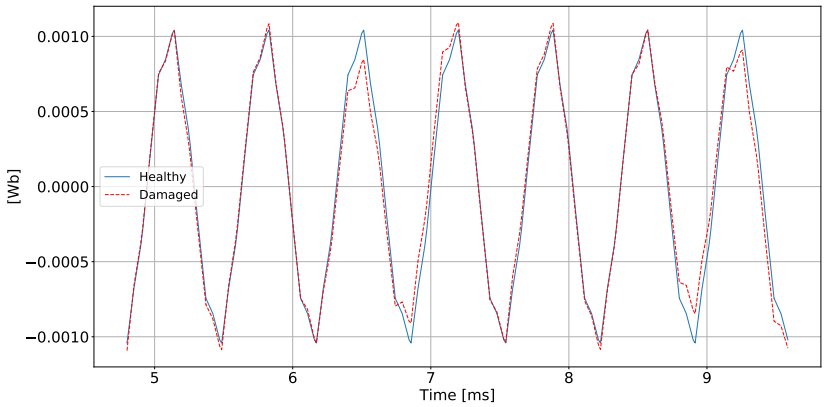

Figure 4.15 Comparison between time variation of phase A flux linkage in BR2804 healthy motor and with a demagnetised magnet along a mechanical turn, at 12500 RPM.

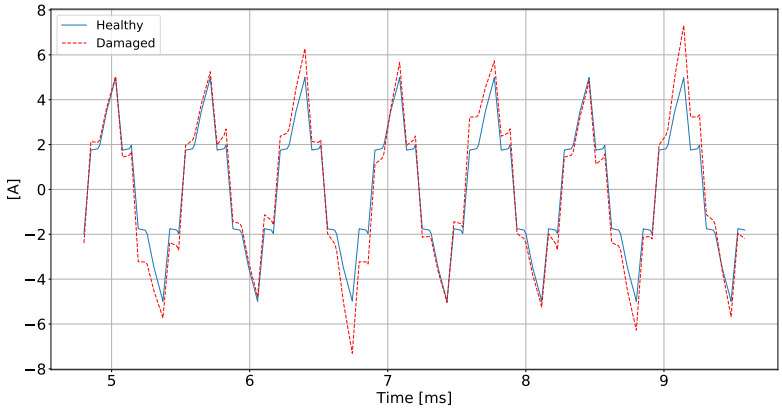

Figure 4.16 Comparison between time variation of phase A current in BR2804 healthy motor and with a demagnetised magnet along a mechanical turn, at 12500 RPM.

for the damaged motor is higher than the one relative to the healthy motor. The increase of the average torque is due to the increased cogging torque, while the peaks anomalies are caused by the current unbalance.

It is important to highlight that the damaged motor would need more current to produce the same torque of the healthy motor; indeed the average torque gets

reduced due to the loss of one magnet, as can be seen from equation (4.1) [22].

$$T = k_T \varphi i \tag{4.1}$$

where:

T =Torque
k_T=Torque Constant
φ =Magnetic Flux

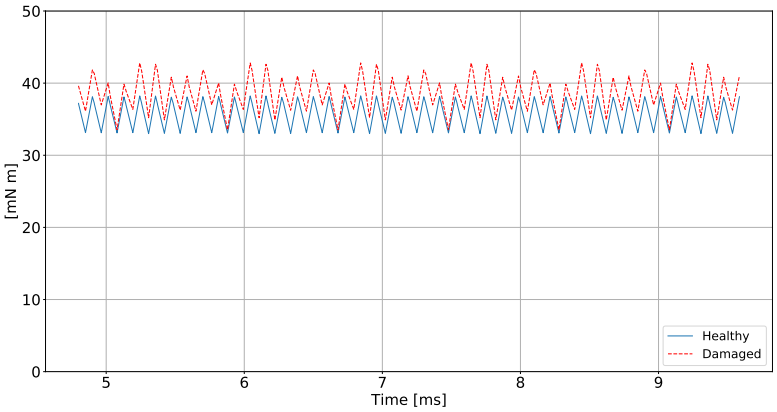

Figure 4.17 Comparison between time variation of torque in BR2804 healthy motor and with a demagnetised magnet along one mechanical turn at 12500 RPM.

Table 4.6 Average Torque Data Comparison along a mechanical turn.

Torque Mean Value		
Healthy	*Damaged*	*Percentage Increase*
36.29 mNm	39.21 mNm	7.458%

4.5 Computing the indicators

Before the execution of the experimental tests, the indicators have been computed on the simulation data. In order to do so, the procedure explained in next chapter (refer to Figure 5.6) has been followed. First of all, the phase voltages have been

acquired for a complete mechanical turn. Then, they have been split in 7 parts, i.e. the number of motor's polepairs. Each chunk represents an electrical turn.

At this point there are 3 groups, one for each phase, containing the phase voltage signals of the 7 electrical turns, exactly the situation depicted in Figure 4.18 and Figure 4.19 respectively for the healthy and demagnetised motor.

By comparing the two sets of figures, it is possible to observe that, while for the healthy case the phase voltages of the electrical turns are completely overlapping, for the demagnetised motor they are different during the non-conducting steps.

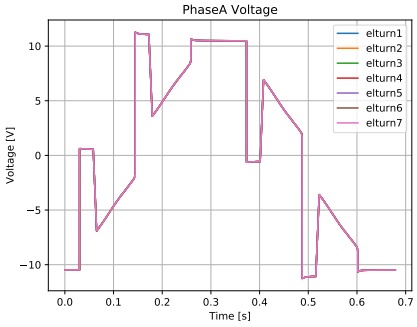

(a) Phase A Voltage.

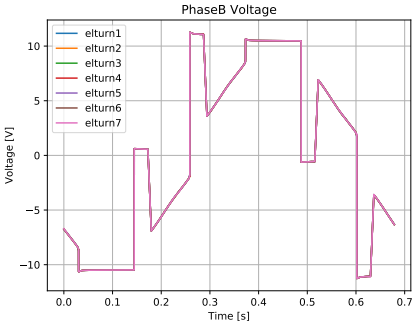

(b) Phase B Voltage.

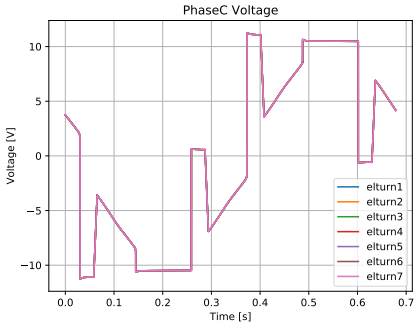

(c) Phase C Voltage.

Figure 4.18 Phase Voltages of the healthy motor - 12500RPM.

It is now possible to compute the indicators i_{xc} and i_{diff}, by following the procedure summarised in 3.14, obtaining the results of Table 4.7.

The indicators correctly shows that the signals relative to electrical turns of the demagnetised motor are more *dissimilar* between them. This result will be checked in the next chapter with the experimental tests.

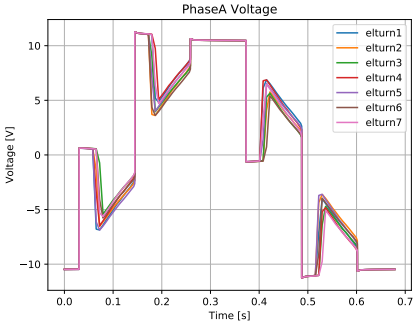

(a) Phase A Voltage.

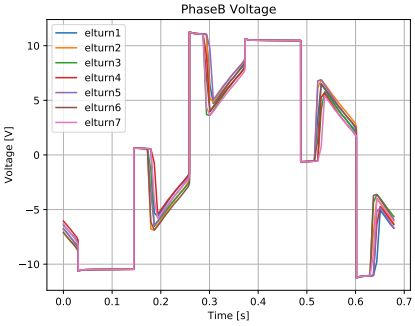

(b) Phase B Voltage.

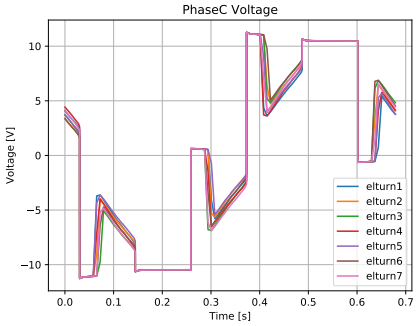

(c) Phase C Voltage.

Figure 4.19 Phase Voltages of the demagnetised motor - 12500RPM.

Table 4.7 Indicators computed from simulation data - 12500RPM.

	Healthy	**Demagnetised**
i_{xc}	62.99	62.44
i_{diff}	2.34	2.42

5 Experimental Results

The experiments have been carried out by using the **P-NUCLEO-IHM001**, a development kit composed by a control board, a power board and a motor (Figure 5.1). This development board facilitated very much the research work,

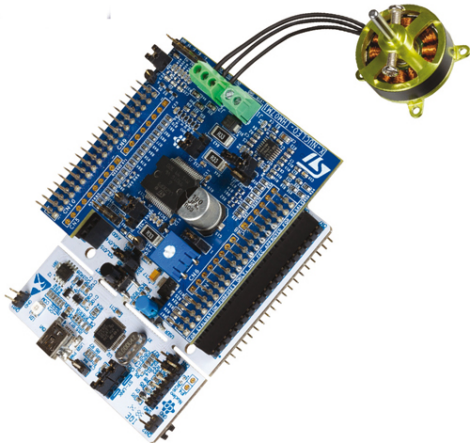

Figure 5.1 P-Nucleo-IMH001 Development kit.

as the variables needed for this study were already available to be read at some board's pin. The datasheet, software and tutorials about the board can be found at [1].

The board is also already prepared to drive the motor in sensor-less mode with two algorithms, *six-step* or *Field Oriented Control (FOC)*, but for this study only the first algorithm has been used.

The motor included in the kit is a quite common type in the radio controlled

modelling world and it has been described in details in § 4.1 during the unmounting procedure.

5.1 Motor Demagnetisation Procedure

To perform the experiments, the motor has been partially demagnetised by removing one of the 14 magnets and replacing it with a block of aluminium of similar weight ($\approx 0.19\,\mathrm{g}$) and size, to avoid the effects of eccentricity caused by weight unbalance on the rotor. The aluminium has been chosen for having a magnetic permeability very similar to the motor magnets (refer to Table 5.1). In this way it has been possible to replicate the effect of a complete loss of the magnetic properties without compromising the balance of the rotor.

Table 5.1 Relative Permeability.

Material	Relative Permeability
Aluminium	**1.000022**
XG128-120	**0.999982**

The magnet has been removed by chemically dissolving the glue which connected it to the rotor and thanks to this procedure, no other parts of the motor have been damaged. The result of this process is shown in Figure 5.2.

(a) (b)

Figure 5.2 Demagnetisation process: rotor with a missing magnet (a), highlighted by the yellow circle, and rotor with the replacement piece of inert material (b), easily recognisable for the red glue.

5.2 Fault Detection on real motor

5.2.1 Data Acquisition and Filtering

The voltage signals have been obtained by measuring with the oscilloscope at the pins correspondent to the signals **BEMF1**, **BEMF2** and **BEMF3** of the P-NUCLEO board, represented in Figure 5.3.

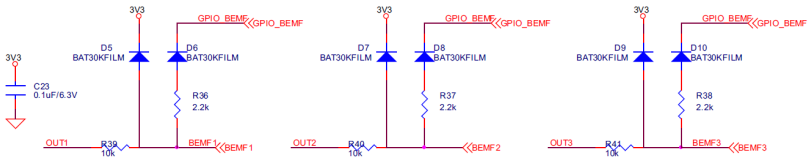

(a) Schematics.

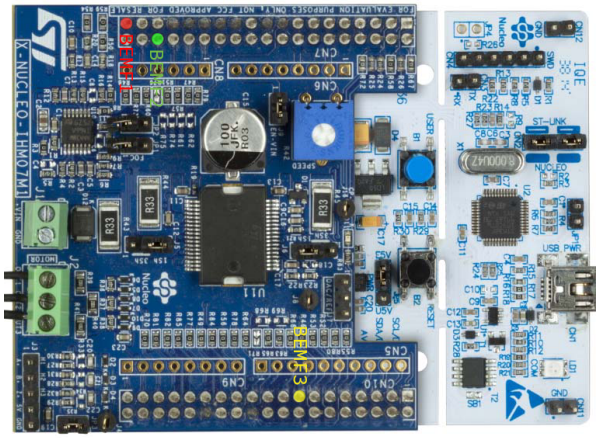

(b) Measuring Pins.

Figure 5.3 P-NUCLEO-IHM001 BEMF acquisition circuit.

The primary role of this circuit is to measure the motor back-EMF by using one of the techniques explained in Appendix A, but in this work the entire phase-phase voltage will be acquired and used.

The voltage signals are clamped to 3.3 V in order to be directly read by the microcontroller's Analog to Digital Converter (ADC).

In Figure 5.4 is shown an acquisition of about 2ms with the motor running at constant speed of 3000 RPM performed with an oscilloscope by measuring at the previously indicated pins. From the figure it is possible to appreciate that the motor is controlled by varying its average voltage with the technique of the Pulse

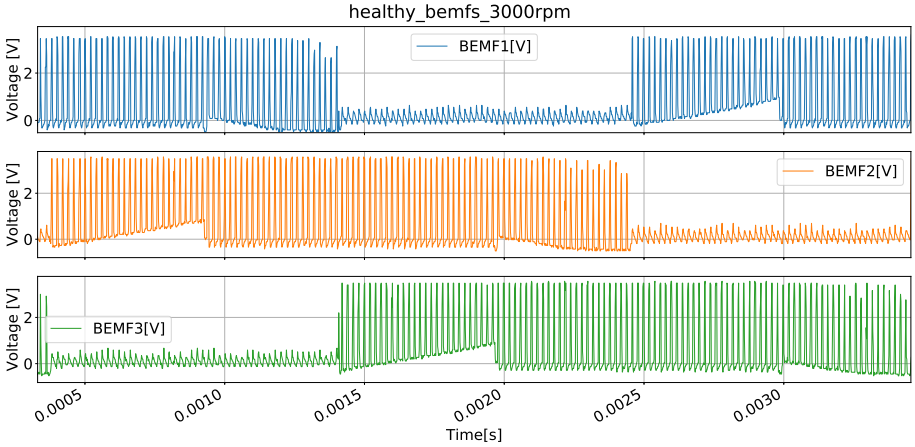

Figure 5.4 Oscilloscope acquisition - 3000RPM.

Width Modulation (PWM), and, in order to apply the proposed technique the signals need to be low filtered.

These phase-phase voltage signals contain both information about the conduction step and the back-EMF. The flux asymmetry along the mechanical turn, generated by the missing magnet, is expected to be reflected on these phase voltage as a dissimilarity between the electrical turns.

In order to avoid misunderstandings, the signals acquired from the previously indicated pins (Figure 5.3) will be named in this work as specified in Table 5.2.

Table 5.2 Acquired signals.

Pin	Name	Unit
BEMF1	PhaseA	Volt
BEMF2	PhaseB	Volt
BEMF3	PhaseC	Volt

The acquired voltage signals are then low filtered with a Butterworth low-pass filter with the cut-off frequency set to the current angular speed multiplied by the number of pole-pairs. The signals resulting from filtering the ones in Figure 5.4 are shown in Figure 5.5.

Table 5.3 summarises the acquisitions, and the relative data, that have been acquired for both the healthy and the partially demagnetised motor at different

Appendix A

Technical Aspects

The back-EMF estimation is an already solved problem and is not the scope of this work, hence the following chapter is just meant to briefly explain the methods used to obtain a reliable measurement of the induced voltage and to provide useful literature references.

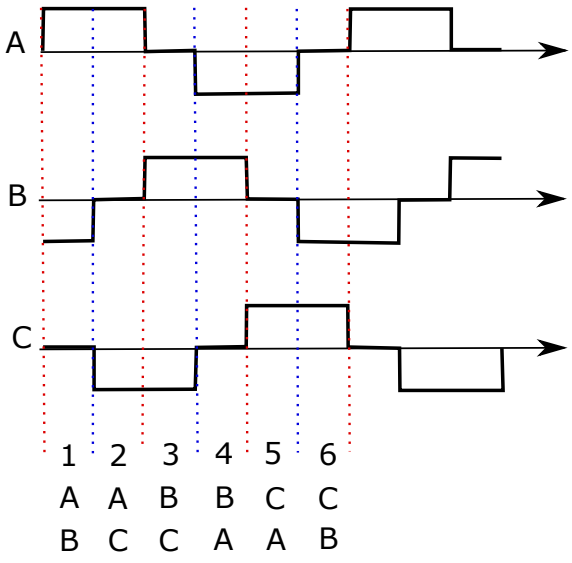

Figure A.1 6-Step Motor Control.

A.1 Six-Step Motor Control

Typically, a Brushless dc motor is driven by a three-phase inverter with six-step commutation as depicted in Figure A.1. The conducting interval for each phase is 120 degE, which represent one step. For each step a combination of transistor is on the conduction state. In order for the motor to move, the commutation shall happen in a given sequence (in the case of Figure A.1 is AB-AC-BC-BA-CA-CB).

From the picture it can be seen that only two phases conduct current at any time, leaving the third phase floating. For example, consider step1 in the Figure A.1:

1. The current is flowing in the winding from the outer to the inner part. This direction produces (by convention) a *North* pole and is considered negative.
2. The current goes from A to B. The current circulating in B produces a *South* pole and is considered negative
3. No current is circulating in phase C. The back-EMF can be measured

During step2 the situation is exactly the same, with the phase A and C in conducting state and phase C floating.

Hence it is possible to sense the back-EMF at any step by considering the non-conducting winding. For an electric turn (six-steps) it is possible to measure the induced voltage on the same winding two times, as can be seen in Figure A.2 [45].

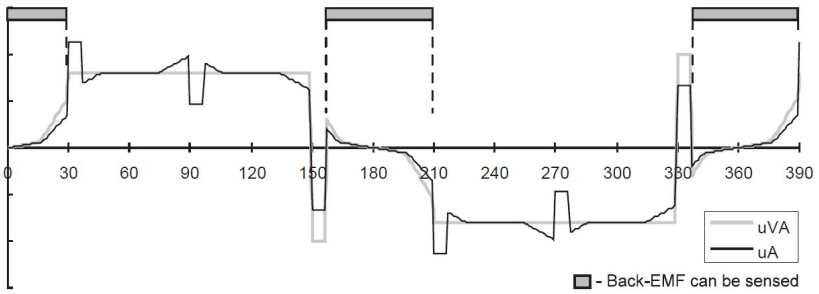

Figure A.2 Phase Voltage Waveforms.

In order to produce maximum torque, the inverter should be commuted every 60 degE so that current is in phase with the back EMF. The commutation timing is determined by the rotor position, which can be detected by a rotor position sensor or estimated from motor parameters, i.e., the back EMF on the floating coil of the motor.

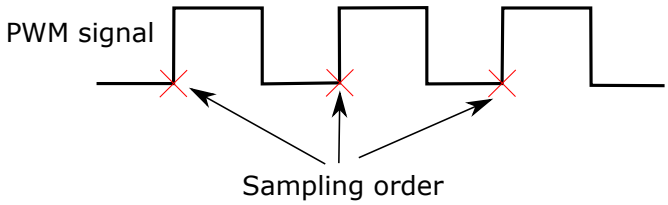

Figure A.3 Back-EMF sampling during PWM OFF state.

A.2 Direct Sensing of the Back-EMF

In this section there is a brief review of the main methods used in the industry to obtain the back-EMF measurement.

An additional difficulty is that the back-EMF is referred to the neutral point, but most of the times this point is not accessible because of delta-wound or simply because the wire is not extracted.

If a PWM switching driver is used, there are two possible moment to measure the induced voltage, i.e. during the PWM **OFF** or **ON** state. Following the technical differences between the two choices are shown, highlighting their advantages and drawbacks. It is important to highlight that the two methods are not exclusive, i.e. both can be implemented to sense the induced voltage during the entire available measurement period, independently from the PWM state. Also, depending on the micro-controller performances, the sampling of the back EMF can be done at higher frequency, allowing for additional filtering and spurious rejection.

A.2.1 PWM OFF state - Resistor Method

This method is a patent of ST MicroElectronics and can be found already implemented in many microcontroller of this brand and explained in different application notes ([57, 56]). The configuration to measure using this technique, as well the measurement instant is shown in Figure A.3.

During the **OFF** state of PWM, the current circulating in active winding of the motor passes through D2, the adjacent diode of switch T1.

Due to the fact that the potential of the neutral point is grounded, the voltage comparator obtains complete information about the back-EMF voltage of the non-energised phase on its input via C ([57]).

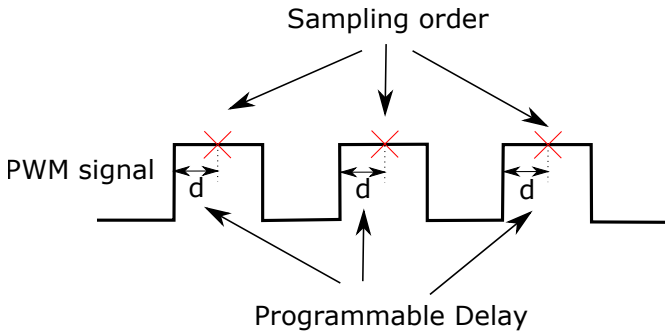

Figure A.4 Back-EMF sampling during PWM ON state.

During step1 the motor equations become:

$$\begin{aligned} v_A^b &= \frac{1}{2} v_{DC} \\ v_B^b &= -\frac{1}{2} v_{DC} \\ i_A &= -i_B \\ i_C &= 0 \\ \mathrm{d}i_C &= 0 \\ e_A + e_B + e_C &= 0 \end{aligned} \tag{A.1}$$

The general expression for computing the induced voltage is:

$$e_i = \frac{2}{3} v_i^b \quad \forall i \in [A,B,C] \tag{A.2}$$

Equation (A.2) **is valid if no current is circulating** in the non-fed phase. To avoid this, a certain time should be waited for the winding to discharge the energy accumulated as inductance during the previous step.

Advantages

This method is already implemented on various industrial and automotive grade micro-controllers and need only three external resistors ([57]). The main advantage of this method is that it does not need any filtering to acquire the induced voltage, giving a signal with a high signal-to-noise ratio and no delay.

Drawbacks

To be implemented, this method need a minimum PWM OFF time to be implemented. This limit the maximum duty cycle and this cannot be acceptable for

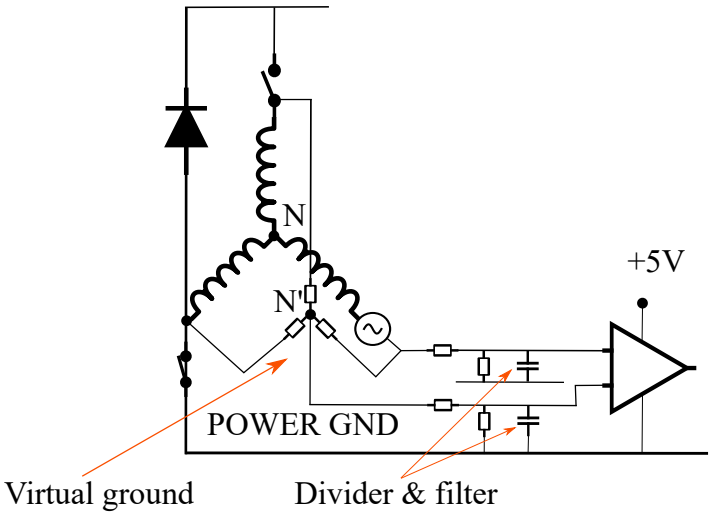

Figure A.5 Implementation of the Classical Method using a Voltage Divider and Filter.

some applications. Also it need the lower part of the bridge to be in **always ON state**.

A.2.2 PWM ON state - Virtual Neutral Point Method

When the PWN is at ON state, the neutral point is not grounded (see the Figure A.4).

Hence, if it is not possible to physically access the neutral point, it shall be virtually recreated with some workaround.

The method proposed by [24] contemplate the use of an additional network, created ad-hoc with three resistors, to obtain the voltage reference of floating phase necessary to perform the back-EMF detection.

If the DC bus is very stable and does not present fluctuations, this additional network can be avoided and the reference neutral point can be fixed at half the DC voltage value.

Due to the presence of superimposed PWM signal, this measurement contain very high common mode voltage and high frequency noise. So voltage dividers and low pass filters are needed to reduce the common mode voltage and smooth the high frequency noise.

This filtering can be done with:

1. Analogue Filter, build with resistors and capacitors

2. Digital Filter, has the advantage to be adapted to the motor speed

This method is explained in detail in [57]

Advantages

This method allows to measure the back-EMF also with a PWM duty cycle of 100%.

Drawbacks

Due to the voltage divider being used to sense back-EMF, this method is less sensitive that the Resistors method. If the DC bus voltage is 300 V, the potential of the neutral point can vary from zero to 300 V. Considering that he allowable common mode voltage for a comparator is typically a few volts, the signal shall be strongly attenuated reducing the signal sensitivity at low speed and especially at start-up, where it is needed the most.

This sampling method is also dependent on the motor speed because the different networks are influenced by back-EMF levels and the components must be sized according to the nominal operation point of the motor. Of course, if using a digital filter, this can be adapted according to the measured motor speed.

List of Figures

List of Tables

Bibliography

[1] *P-nucleo-ihm001*, https://www.st.com/en/evaluation-tools/p-nucleo-ihm001.html, Accessed: 2018-11-09.

[2] W. Abed, S. Sharma, R. Sutton, and A. Motwani, *A robust bearing fault detection and diagnosis technique for brushless dc motors under non-stationary operating conditions*, Control, Automation and Electrical Systems **26** (2015), no. 3, 241–254.

[3] H. Abu-Rub, S. M. Ahmed, A. Iqbal, H. A. Toliyat, and M. M. Rahimian, *Incipient bearing fault detection for three-phase brushless dc motor drive using anfis*, IEEE International Symposium on Diagnostics for Electric Machines, Power Electronics & Drives, IEEE, 2011, pp. 620–625.

[4] K. Ahsanullah, E. Jeyasankar, A. Vignesh, S. Panda, R. Shanmukha, and S. Nadarajan, *Eccentricity fault analysis in pmsm based marine propulsion motors*, 20th International Conference on Electrical Machines and Systems, IEEE, 2017, pp. 1–6.

[5] M. Akar, M. Hekim, and U. Orhan, *Mechanical fault detection in permanent magnet synchronous motors using equal width discretization-based probability distribution and a neural network model*, Electrical Engineering & Computer Sciences **23** (2015), no. 3, 813–823.

[6] J Arellano-Padilla, M Sumner, and C Gerada, *Winding condition monitoring scheme for a permanent magnet machine using high-frequency injection*, IET Electric power applications **5** (2011), no. 1, 89–99.

[7] PS Barendse and P Pillay, *A new algorithm for the detection of faults in permanent magnet machines*, IEEE Industrial Electronics, IECON 2006-32nd Annual Conference on, IEEE, 2006, pp. 823–828.

[8] Debasmita Basak, Arvind Tiwari, and S. P. Das, *Fault diagnosis and condition monitoring of electrical machines - A review*, Proceedings of the IEEE International Conference on Industrial Technology,Mumbai, India (2006), 3061–3066.

[9] A. Bellini, F. Filippetti, C. Tassoni, and G.-A. Capolino, *Advances in diagnostic techniques for induction machines*, IEEE Transactions on Industrial Electronics **55** (2008), 4109–4126, cited By (since 1996) 179.

[10] Romain Breuneval, Guy Clerc, Babak Nahid-Mobarakeh, and Badr Mansouri, *Hybrid diagnosis of intern-turn short-circuit for aircraft applications using svm-mbf*, Fuzzy Systems (FUZZ-IEEE), 2017 IEEE International Conference on, IEEE, 2017, pp. 1–6.

[11] Subhadeep Chakraborty, Eric Keller, Asok Ray, and Jeffrey Mayer, *Detection and estimation of demagnetization faults in permanent magnet synchronous motors*, Electric Power Systems Research **96** (2013), 225–236.

[12] Ferhat Çira, Müslüm Arkan, and Bilal Gümüş, *A new approach to detect stator fault in permanent magnet synchronous motors*, Diagnostics for Electrical Machines, Power Electronics and Drives (SDEMPED), 2015 IEEE 10th International Symposium on, IEEE, 2015, pp. 316–321.

[13] Bashir Mahdi Ebrahimi and Jawad Faiz, *Feature extraction for short-circuit fault detection in permanent-magnet synchronous motors using stator-current monitoring*, IEEE Transactions on Power Electronics **25** (2010), no. 10, 2673–2682.

[14] BM Ebrahimi, J Faiz, and BN Araabi, *Pattern identification for eccentricity fault diagnosis in permanent magnet synchronous motors using stator current monitoring*, IET electric power applications **4** (2010), no. 6, 418–430.

[15] Jawad Faiz and Ehsan Mazaheri-Tehrani, *A novel demagnetization fault detection of brushless DC motors based on current time-series features*, 2017 IEEE 11th International Symposium on Diagnostics for Electrical Machines, Power Electronics and Drives (SDEMPED), 2017, pp. 160–166.

[16] Jacek F. Gieras, *Permanent Magnet Motor Technology Design and Applications*, 2010.

[17] Bon-Gwan Gu, *Study of ipmsm interturn faults part ii: Online fault parameter estimation*, IEEE Transactions on Power Electronics **31** (2016), no. 10, 7214–7223.

[18] Reemon Z Haddad and Elias G Strangas, *Fault detection and classification in permanent magnet synchronous machines using fast fourier transform and linear discriminant analysis*, Diagnostics for Electric Machines, Power Electronics and Drives (SDEMPED), 2013 9th IEEE International Symposium on, IEEE, 2013, pp. 99–104.

[19] Duane C Hanselman, *Brushless permanent magnet motor design*, 2006.

[20] Mehrdad Heydarzadeh, Mohsen Zafarani, Bilal Akin, and Mehrdad Nourani, *Automatic fault diagnosis in pmsm using adaptive filtering and wavelet transform*, Electric Machines and Drives Conference (IEMDC), 2017 IEEE International, IEEE, 2017, pp. 1–7.

[21] Mehrdad Heydarzadeh, Mohsen Zafarani, Enes Ugur, Bilal Akin, and Mehrdad Nourani, *A model-based signal processing method for fault diagnosis in pmsm machine*, Energy Conversion Congress and Exposition (ECCE), 2017 IEEE, IEEE, 2017, pp. 3160–3164.

[22] Austin Hughes and Bill Drury, *Electric Motors and Drives*, 4th ed., Elsevier, 2013.

[23] C. Ierardi, L. Orihuela, and I. Jurado, *Guidelines for a systematic review in systems and automatic engineering. Case study: distributed estimation techniques for cyber-physical systems*, European Control Conference (Limassol, Cyprus), June 2018, pp. 2230–2235.

[24] Kenichi Iizuka, Hideo Uzuhashi, Minoru Kano, Tsunehiro Endo, and Katsuo Mohri, *Microcomputer Control for Sensorless Brushless Motor*, IEEE Transactions on Industry Applications **IA-21** (1985), no. 3, 595–601.

[25] Rolf Isermann, *Fault-diagnosis systems: An introduction from fault detection to fault tolerance*, 2006.

[26] Hyeyun Jeong, Seokbae Moon, Jewon Lee, and Sang Woo Kim, *Inter-turn short fault diagnosis of permanent magnet synchronous machines using negative sequence components*, Industrial Technology (ICIT), 2016 IEEE International Conference on, IEEE, 2016, pp. 170–174.

[27] K-H Kim, B-G Gu, and I-S Jung, *Online fault-detecting scheme of an inverter-fed permanent magnet synchronous motor under stator winding shorted turn and inverter switch open*, IET electric power applications **5** (2011), no. 6, 529–539.

[28] B. Kitchenham and S. Charters, *Guidelines for performing systematic literature reviews in software engineering*, EBSE Technical Report, 2007, pp. 1–65.

[29] Ramu Krishnan, *Permanent Magnet Synchronous and Brushless DC Motor Drives*, 2010.

[30] W. le Roux, R. G. Harley, and T. G. Habetler, *Rotor fault analysis of a permanent magnet synchronous machine*, Proc. 15th Int. Conf. Elect. Mach. (ICEM'02) (2002).

[31] Nicolas Leboeuf, Thierry Boileau, Babak Nahid-Mobarakeh, Guy Clerc, and Farid Meibody-Tabar, *Real-time detection of interturn faults in pm drives using back-emf estimation and residual analysis*, IEEE Transactions on Industry Applications **47** (2011), no. 6, 2402–2412.

[32] Seung-Tae Lee, Kyung-Tae Kim, and Jin Hur, *Diagnosis technique for stator winding inter-turn fault in bldc motor using detection coil*, Power Electronics and ECCE Asia (ICPE-ECCE Asia), 2015 9th International Conference on, IEEE, 2015, pp. 2925–2931.

[33] Manuel A Mazzoletti, Guillermo R Bossio, Cristian H De Angelo, and Diego R Espinoza-Trejo, *A model-based strategy for interturn short-circuit fault diagnosis in pmsm*, IEEE Transactions on Industrial Electronics **64** (2017), no. 9, 7218–7228.

[34] Christelle Piantsop Mbo'o and Kay Hameyer, *Fault diagnosis of bearing damage by means of the linear discriminant analysis of stator current features from the frequency selection*, IEEE Transactions on Industry Applications **52** (2016), no. 5, 3861–3868.

[35] T. J. E. Miller, *Brushless Permanent-Magnet and Reluctance Motor Drives (Monographs in Electrical and Electronic Engineering 21)*, no. 21, 1989.

[36] D. Moher, A. Liberati, J. Tetzlaff, and D.G. Altman, *Reprint-preferred reporting items for systematic reviews and meta-analyses: the PRISMA statement*, Physical Therapy **89** (2009), no. 9, 873–880.

[37] Seokbae Moon, Hyeyun Jeong, Hojin Lee, and Sang Woo Kim, *Interturn short fault diagnosis in a pmsm by voltage and current residual analysis with the faulty winding model*, IEEE Transactions on Energy Conversion **33** (2018), no. 1, 190–198.

[38] Seokbae Moon, Jewon Lee, Hyeyun Jeong, and Sang Woo Kim, *Demagnetization fault diagnosis of a pmsm based on structure analysis of motor inductance*, IEEE Transactions on Industrial Electronics **63** (2016), no. 6, 3795–3803.

[39] SS Moosavi, A Djerdir, Y Ait-Amirat, and DA Khaburi, *Ann based fault diagnosis of permanent magnet synchronous motor under stator winding shorted turn*, Electric Power Systems Research **125** (2015), 67–82.

[40] Subhasis Nandi, Hamid A. Toliyat, and Xiaodong Li, *Condition monitoring and fault diagnosis of electrical motors - A review*, IEEE Transactions on Energy Conversion **20** (2005), no. 4, 719–729.

[41] Yaw D Nyanteh, Sanjeev K Srivastava, Chris S Edrington, and David A Cartes, *Application of artificial intelligence to stator winding fault diagnosis in permanent magnet synchronous machines*, Electric Power Systems Research **103** (2013), 201–213.

[42] Najla Haje Obeid, Alexandre Battiston, Thierry Boileau, and Babak Nahid-Mobarakeh, *Early intermittent interturn fault detection and localization for a permanent magnet synchronous motor of electrical vehicles using wavelet transform*, IEEE Transactions on Transportation Electrification **3** (2017), no. 3, 694–702.

[43] Olivier Ondel, Emmanuel Boutleux, and Guy Clerc, *Diagnosis by pattern recognition for pmsm used in more electric aircraft*, IECON 2011-37th Annual Conference on IEEE Industrial Electronics Society, IEEE, 2011, pp. 3452–3458.

[44] Yonghyun Park, Daniel Fernandez, Sang Bin Lee, Doosoo Hyun, Myung Jeong, Suneel Kumar Kommuri, Changhee Cho, David Reigosa, and Fernando Briz, *On-line detection of rotor eccentricity for pmsms based on hall-effect field sensor measurements*, Energy Conversion Congress and Exposition (ECCE), 2017 IEEE, IEEE, 2017, pp. 4678–4685.

[45] Libor Prokop and Leos Chalupa, *AN1913 - 3-Phase BLDC Motor Control with Sensorless Back EMF Zero Crossing Detection Using 56F80x*, Application Note (2005), no. Freescale Semiconductor, 17–18.

[46] J Quiroga, DA Cartes, CS Edrington, and Li Liu, *Neural network based fault detection of pmsm stator winding short under load fluctuation*, Power Electronics and Motion Control Conference, 2008. EPE-PEMC 2008. 13th, IEEE, 2008, pp. 793–798.

[47] Satish Rajagopalan, *Detection of Rotor and Load Faults in Brushless DC Motors Operating Under Stationary and Non-stationary Conditions*, (2005).

[48] Satish Rajagopalan, Jos M Aller, Jos A Restrepo, Thomas G Habetler, and Ronald G Harley, *Detection of rotor faults in brushless dc motors operating under nonstationary conditions*, IEEE Transactions on Industry Applications **42** (2006), no. 6, 1464–1477.

[49] J Rosero, J Cusido, A Garcia, L Romeral, and JA Ortega, *Detection of stator short circuits in pmsm by mean of joint time-frequency analysis*, Diagnostics for Electric Machines, Power Electronics and Drives, 2007. SDEMPED 2007. IEEE International Symposium on, IEEE, 2007, pp. 420–425.

[50] ———, *Fault detection of eccentricity by means of joint time-frequency analysis in pmsm under dynamic conditions*, Intelligent Signal Processing, 2007. WISP 2007. IEEE International Symposium on, IEEE, 2007, pp. 1–6.

[51] J Rosero, J Cusido, JA Ortega, L Romeral, and A Garcia, *Pmsm bearing fault detection by means of fourier and wavelet transform*, Industrial Electronics Society, 2007. IECON 2007. 33rd Annual Conference of the IEEE, IEEE, 2007, pp. 1163–1168.

[52] J.-R.R. Ruiz, J.A. Rosero, A.G. Espinosa, and L. Romeral, *Detection of Demagnetization Faults in Permanent-Magnet Synchronous Motors Under Nonstationary Conditions*, Magnetics, IEEE Transactions on (2009).

[53] Ali Sarikhani and Osama A Mohammed, *Inter-turn fault detection in pm synchronous machines by physics-based back electromotive force estimation*, IEEE Transactions on Industrial Electronics **60** (2013), no. 8, 3472–3484.

[54] R.R. Schoen, T.G. Habetler, F. Kamran, and R.G. Bartfield, *Motor bearing damage detection using stator current monitoring*, Industry Applications, IEEE Transactions on (1995).

[55] Bhaskar Sen and Jiabin Wang, *Stator interturn fault detection in permanent-magnet machines using pwm ripple current measurement*, IEEE Transactions on Industrial Electronics **63** (2016), no. 5, 3148–3157.

[56] ST Microelectronics, *AN1130 - An Introduction To Sensorless Brushless Dc Motor Drive Applications With the ST72141*, Application Note, 1–29.

[57] _____, *AN1946 - Sensorless Bldc Motor Control and Bemf Sampling Methods With ST7MC*, Application Note (2010), 1–35.

[58] S. Tanimoto and S. Mayumi, *Permanent magnet motor*, (1994).

[59] Peter Tavner and Jim Penman, *Condition Monitoring of Electrical Machines*, (1987), no. January 2012.

[60] P.J. Tavner, *Review of condition monitoring of rotating electrical machines*, IET Electric Power Applications **2** (2008), no. 4, 215.

[61] Julio-César Urresty, Jordi-Roger Riba, and Luis Romeral, *Diagnosis of interturn faults in pmsms operating under nonstationary conditions by applying order tracking filtering*, IEEE Transactions on Power Electronics **28** (2013), no. 1, 507–515.

[62] Min Zhu, Wensong Hu, and Narayan C Kar, *Torque-ripple-based interior permanent-magnet synchronous machine rotor demagnetization fault detection and current regulation*, IEEE Transactions on Industry Applications **53** (2017), no. 3, 2795–2804.